Quantifying Baseflow Using Groundwater Levels in the Upper Colorado River Basin

Nicholas L. Ayres

University of Colorado Boulder
Department of Geological Sciences

Submission: April 4, 2024

A thesis submitted to the Honors Department and the Department of Geological Sciences at the University of Colorado Boulder in partial fulfillment of the requirements for graduation with honors.

Primary Advisor: Shemin Ge: Department of Geological Sciences

Committee Members:

Brian Hynek: Department of Geological Sciences

William Travis: Department of Geography

ABSTRACT

Quantifying Baseflow Using Groundwater Levels in the Upper Colorado River Basin

The vitality of the Colorado River faces significant uncertainty in light of frequent and prolonged droughts induced by climate change. Progressing knowledge concerning the role of groundwater and surface water interactions is critical in informing water resource managers and ultimately easing tension among Colorado River water users—namely, the mechanism of baseflow accounts for a substantial portion of streamflow. Baseflow is considered a proxy for groundwater discharge to streams. Groundwater is vital in sustaining streamflow via baseflow, particularly during periods of low precipitation and overland flow. Previous baseflow studies within the Upper Colorado River Basin discern that more than half of streamflow is accounted for by baseflow. This study aims to quantify baseflow to the Roaring Fork River, a major tributary within the Upper Colorado River Basin. The Roaring Fork River flows along the western margins of Colorado's Southern Rocky Mountains physiographic province.

This study employed an approach based on groundwater level data from the Colorado Division of Water Resources (CDWR). Groundwater level observations were compiled between 2000 and 2022 from over 150 wells in the Roaring Fork subbasin to ultimately interpolate static groundwater level elevations. Hydraulic gradients near the Roaring Fork River were elucidated from contoured groundwater levels. Existing estimates of hydraulic conductivity were analyzed using empirical pumping test formulae. On the basis of averaged hydraulic gradient and hydraulic conductivity, a groundwater discharge of 1.57 m^3/s to the Roaring Fork River is estimated. In parallel, baseflow separation via a graphical method was conducted, which yields a similar magnitude of baseflow to that of the groundwater level approach. This study, for the first

time, demonstrates the potential of utilizing existing groundwater level data to supplement the study of baseflow. Enriching the arsenal of baseflow analysis will help contribute to sustainable and informed water resource management.

ACKNOWLEDGMENTS

This thesis is a product of the inspiration instilled in me by the incredible faculty at the University of Colorado Boulder. Foremost, I would like to thank my advisor, Shemin Ge for her guidance and encouragement. She has been an invaluable mentor throughout my undergraduate tenure by providing me with research ideas, feedback, and direction. I am deeply thankful for her welcomeness and patience.

I would also like to thank the rest of my thesis committee, Brian Hynek, who helped my GIS skills flourish, and William Travis, whose knowledge deepened my passion for studying the arid American West. They were always helpful, and I would like to thank them for their availability throughout this process. Thank you to Scott Stokes and Corrine Liu, graduate students in Dr. Ge's hydrogeology lab, for their assistance, which greatly bolstered my research.

I dedicate this work to my parents Michael and Silvia Ayres and thank them for their support and inspiration. Thank you for sharing your passion for geology and Western landscapes with me.

TABLE OF CONTENTS

FIGURES AND TABLES

I. INTRODUCTION

a. <u>Background</u>

The Colorado River is the lifeblood of the arid and semiarid American West. The Colorado River and its tributaries supply 40 million people with municipal water and irrigate nearly 5.5 million acres of land (U.S. Bureau of Reclamation, 2012). Rapidly declining pool levels in the system's principal reservoirs of Lake Powell and Lake Mead depict a state of ailment for the river, as consumptive use currently outweighs supply. The imbalances between water supply and demand within the Colorado River Basin are projected to reach 4×10^9 m^3 by the year 2060 (U.S. Bureau of Reclamation, 2012). This imbalance largely derives from a projected decrease in overland flow induced by climate change, with estimates reaching a 50% reduction in annual streamflow at the Lee's Ferry outlet (Ficklin et al., 2013). Litigation and water resource management in the basin primarily monitor reservoir storage to assess water availability, including the basin's principal governing documents: the 2007 Interim Guidelines and the 2019 Drought Contingency Plan (U.S. Bureau of Reclamation, 2019). For a more holistic approach to monitoring the vitality of the Colorado River Basin, water resource managers must consider the mechanisms sustaining streamflow, including those pertaining to groundwater-surface water interactions.

The period of receding stream discharge during a period of no excess precipitation is referred to as baseflow (Fetter, 2022). During this period, baseflow is considered a proxy for groundwater discharge to streams and the discharge is composed entirely of groundwater contributions. Baseflow integrates groundwater from multiple flow paths at varying scales, including deep regional groundwater and shallow near-stream flow paths (Miller et al., 2014). The process of separating hydrograph components such as baseflow and runoff is referred to as hydrograph separation (Freeze and Cherry, 1979). Methods of hydrograph separation vary in complexity,

from graphical recession curve approaches that separate the runoff and baseflow components of a hydrograph (Barnes, 1939), digital filter methods (Nathan and McMahon, 1990), and chemical mass balance hydrograph separation methods (Pinder and Jones, 1969). In the Upper Colorado River Basin (UCRB), a chemical mass balance method that employs specific conductance data as the chemical constituent for chemical mass balance hydrograph separation has been implemented by Miller et al. (2014) and later by Rumsey et al. (2015). A comparative study of seven commonly used graphical hydrograph separation methods discerned that Eckhardt's recursive digital filter method (Eckhardt, 2005) is the most hydrologically plausible algorithm and can be applied to hydrographs of any temporal length (Eckhardt, 2008). Studies from both Miller et al. (2014) and later by Rumsey et al. (2015) estimate that approximately half of streamflow in the UCRB originated as baseflow.

b. Study Area

The Roaring Fork Watershed is located along the western margins of Colorado's Southern Rocky Mountains and drains the Sawatch, Collegiate, and Elk Ranges (Figure 1). The 3760 km^2 watershed is characterized by snowmelt-dominated hydrology and is a major tributary of the UCRB. The highest point, Castle Peak, has an elevation of 4,348 m, and the lowest point, the confluence of the Colorado and Roaring Fork Rivers, lies at 1,803 m. Elevation gradients for the Roaring Fork River range between 1.5 and 15 m / km (Roaring Fork Conservancy, 2007). The Fryingpan-Arkansas Project diverts 1.3 x 10^8 m^3 / year of water via a transmountain diversion tunnel from the Roaring Fork River to the Arkansas River. Sanderson et al. (2011) estimate that the transmountain diversion accounts for an 18% reduction in flow relative to natural conditions. The chief tributary stream of the Roaring Fork River is the Fryingpan River, which contains the

only major water storage unit in the Roaring Fork Watershed, Reudi Dam, and reservoir. Notable hydrologic monitoring networks within the watershed include the United States Geological Survey stream gauging network, the Roaring Fork Observation Network (iRON), and the Colorado Division of Water Resources (CDWR) well permit database. The city of Aspen, the principal municipality of the Roaring Fork Watershed is located in the valley of the Roaring Fork River.

Previous studies of baseflow in the UCRB identified that baseflow yield is enhanced in high-elevation watersheds (Rumsey et al., 2015). This study employs the Roaring Fork Watershed as a case study for studying the mechanism of baseflow in high-elevation watersheds in the UCRB. The Roaring Fork Watershed makes for a suitable study area in that it is mostly decoupled from flow alteration and has a comparatively high density of groundwater wells relative to other UCRB watersheds.
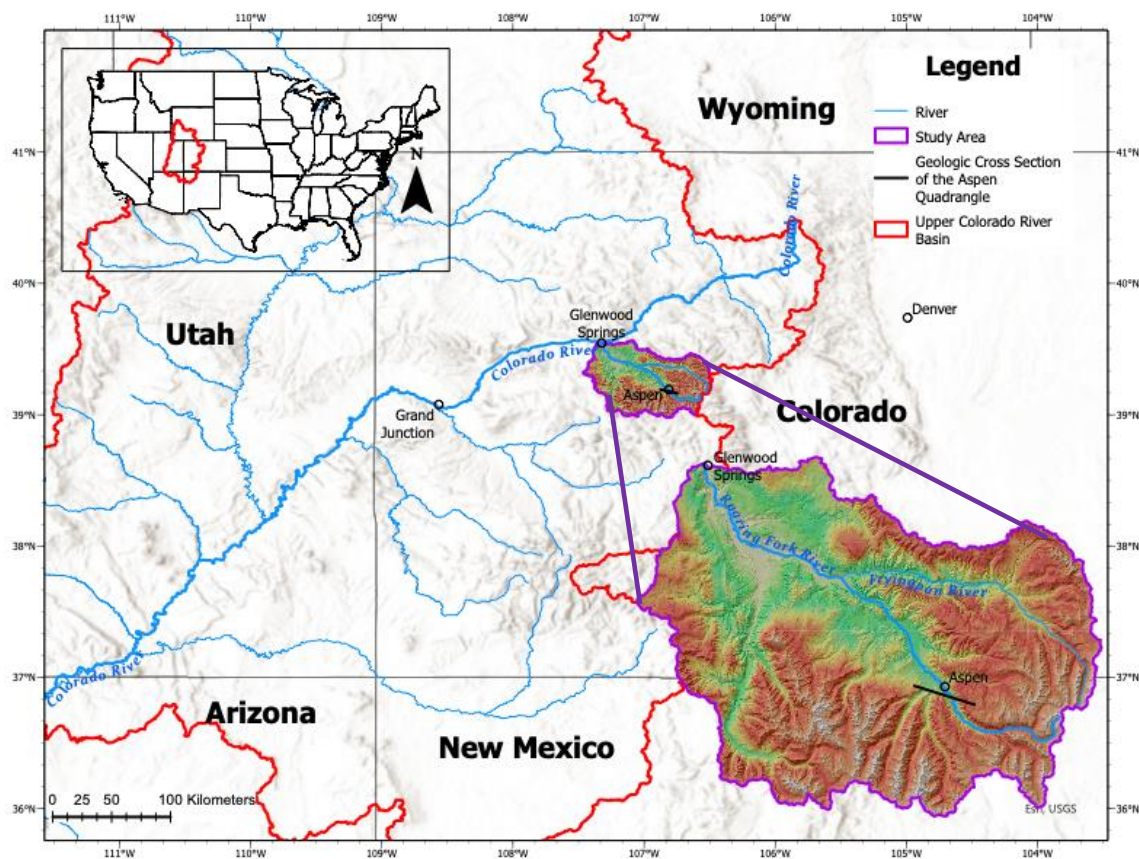
Figure 1. Map of the Roaring Fork Watershed study area. Notable features include major streams in the Upper Colorado River Basin (blue), and the transect for the Geologic Cross Section of the Aspen Quadrangle (black) (Figure 2). Watershed is defined by USGS HUC 8 Boundaries.

c. Purpose of This Study

This study aims to quantify groundwater's role in sustaining the streamflow of the Roaring Fork River, to serve as an analog for other high-elevation watersheds in the UCRB. Although it is well established that the contribution of baseflow to streamflow is substantial, the quantity of baseflow is rarely quantified in the UCRB and the mechanism is largely understudied. The streamflow parameter of baseflow is especially hard to quantify, as there are currently no in-situ measurements that directly relate to baseflow. Without a comprehensive understanding of baseflow, which accounts for about half of streamflow, water supply estimates in the UCRB will

have limitations. Most literature concerning baseflow in the UCRB uses some variety of hydrograph separation methods (Swanson et al, 2020), (Miller et al., 2014), (Rumsey et al., 2015).

This study investigates an alternative approach to quantifying baseflow: employing physical groundwater level data compiled from 151 wells in the CDWR well-permitting database. Groundwater levels were interpolated and visualized in ArcGIS Pro to estimate hydraulic gradients in application to Darcy's law. Results were compared to Eckhardt's recursive digital filter, which was conducted in concert. With the ever-expanding United States Geological Survey (USGS) National Ground-Water Monitoring Network (NGWMN), which has a cumulative network of 17,654 water-level wells and 4,114 water-quality wells, groundwater data is increasingly available (NGWMN, 2024). This method, which to current knowledge has not yet been implemented in baseflow study, is cost-effective compared to existing methods and has a physical basis that is not yet seen in the baseflow literature. Although methods such as specific conductance accurately inform baseflow parameters, they are resource-intensive and add to the routine maintenance of a gaging station, making them site-limited.

The principal inquiries motivating this study are *1) How important is groundwater's role in sustaining streamflow?* and *2) Does the groundwater level method provide a frugal complement to existing methods of quantifying baseflow?*

II.   STUDY SITE DESCRIPTION

a.   <u>Geologic Setting of the Roaring Fork Watershed</u>

Within the Roaring Fork Watershed, lies the intersection of the Colorado mineral belt and the west margin of the north-trending Sawatch uplift, Laramide in age. Generally, the basin consists of a Precambrian basement overlain by a thin shelf sequence of Cambrian to Mississippian aged sedimentary rock, characteristic of thin-skinned deformation (Bryant and Freeman, 1977). In this regard, the Aspen quadrangle is a geologically unique locality within the broader southern Rocky Mountains, which rarely contains exposed sedimentary strata at such elevations. Two principal structural features within the Aspen quadrangle are the Aspen Mountain Syncline and the Castle Creek Fault Zones, both Laramide features, shown in Figure 2. The Castle Creek Fault Zone, a product of the Sawatch uplift, exhibits a stratigraphic separation of 4.2 km (Bryant and Freeman, 1977).

The region's geologic history accounts for a complex hydrogeologic framework. The primary hydrogeologic units within the basin are 1) unconsolidated Quaternary units, mostly Holocene alluvium, and Pleistocene glacial deposits, and 2) pre-Quaternary bedrock units, primarily of the Minturn, Maroon, and Entrada Formations. An average alluvial thickness of 40 meters for the Roaring Fork Valley is gleaned from borehole lithology data, with the upper half mostly containing large boulder clasts (CDWR, 2023). Due to structures such as the Castle Creek Fault Zone, there is a high occurrence of fault zone-enhanced aquifers, which may impede or conduit groundwater (Kolm and van der Heijde, 2011).

The landscape morphology is largely defined by glacial processes. The larger mountain valleys are glacial troughs later incised and modified by fluvial erosion. Most glacial landforms in the watershed were deposited during the Last Glacial Maximum (~20 ka) (Birkeland, 1973).

Lower parts of the Roaring Fork Valley contain large sequences of glacial moraine and outwash deposits, up to 200 m in thickness. Within the Roaring Fork Valley, surficial deposits overly a Precambrian quartz monzonite pluton. Active rock glaciers are abundant in the watershed, including the extensively studied Mt. Sopris rock glacier, which is about 2 km in length with a 25 m tall terminus (Anderson, 2023).
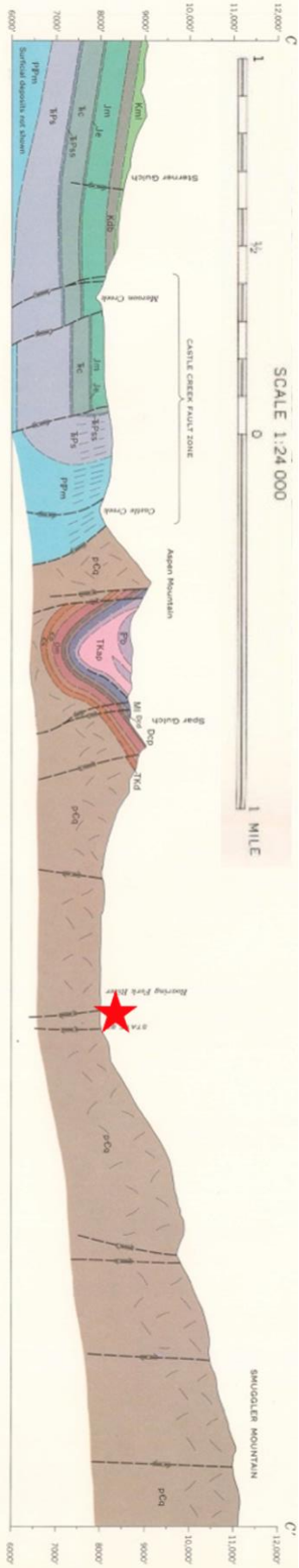
Figure 2. Geologic cross section of the Aspen quadrangle. Key structural features include the Aspen Mountain Syncline and the Castle Creek Fault Zone, both Laramide features. In many stream reaches, surficial deposits overly quartz monzonite. The transect for the cross-section is shown in Figure 1. The red star references the location of the Roaring Fork River (Modified from Bryant, 1971).

    b.   Hydroclimate of the Roaring Fork Watershed

Due to the extreme elevation gradient present in the watershed, the climate varies significantly from the alpine to the montane zones. The average annual precipitation in Aspen (2,410 m) is about 48 cm per year (O'Keefe and Hoffman, 2007). The average annual max and min temperatures for Aspen are 13.2 °C and -3.5 °C, respectively. The climograph for NOAA station Aspen 1 SW, CO (Figure 3) gleans that most precipitation comes in the spring. On Independence Pass (3,218 m), the headwaters of the Roaring Fork River, the average annual precipitation is 75.7 cm per year. The majority of the precipitation in the alpine is delivered via snowfall, with an average cumulative snowfall of 858.3 cm / year on Independence Pass.
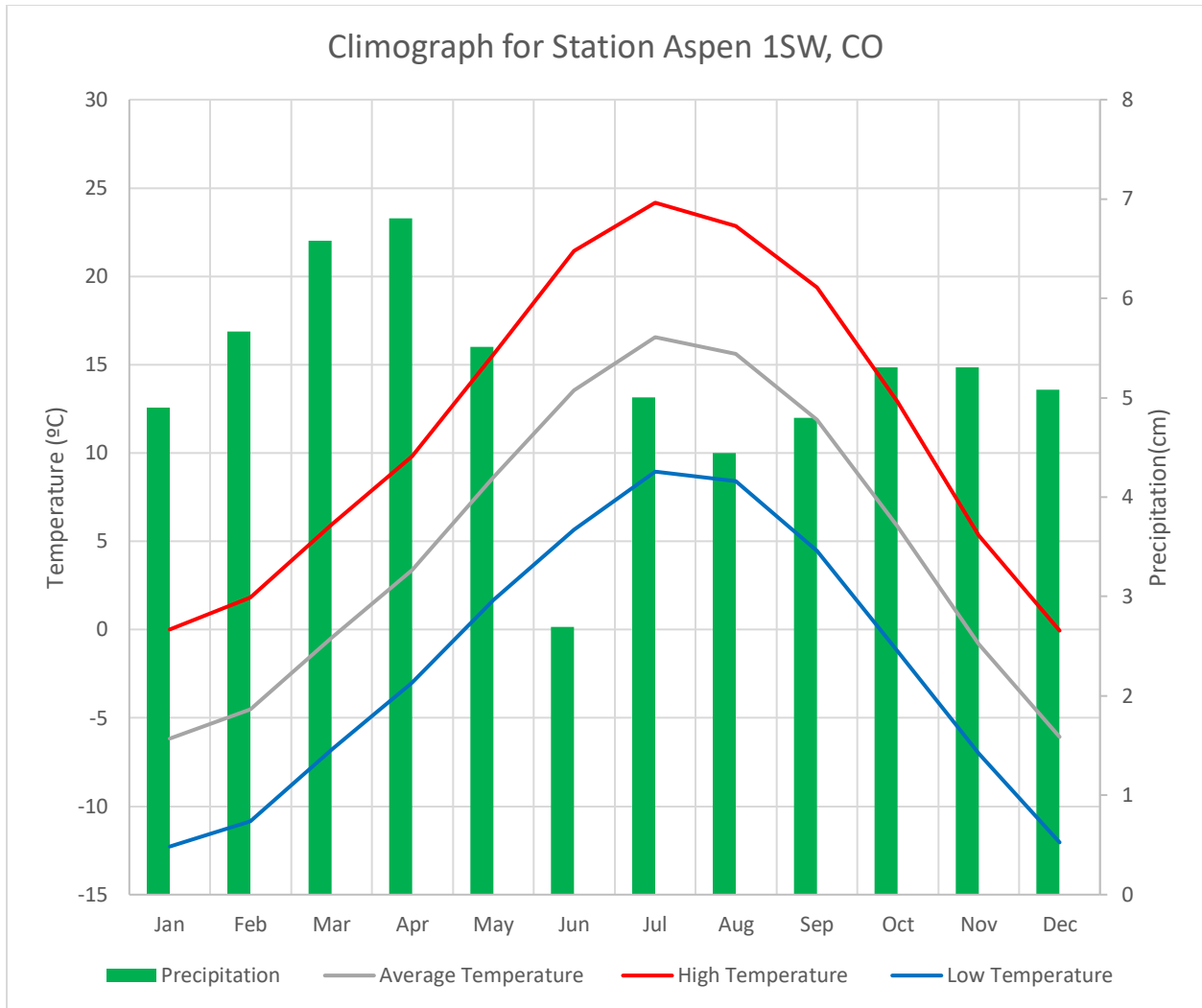
Figure 3. Climograph for NOAA Station Aspen 1 SW, CO US (8175 ft). Based on monthly normals collected from 1991-2023. Precipitation reaches a maximum in April, while temperatures climax in July (NOAA NCEI, 2023).

c. Spatiotemporal Analysis of Soil Moisture

Soil moisture is an excellent proxy for hydroclimatic conditions, which is the basis of the

Roaring Fork Observation Network (iRON). iRON, comprised of 10 soil moisture stations

operated by the Aspen Global Change Institute (AGCI), is a long-term research program aiming

to investigate the relationship between watershed dynamics in a changing climate (AGCI, 2023).

To investigate seasonal dynamics in the Roaring Fork Watershed, this study conducted a

spatiotemporal analysis of soil moisture, employing recurrent soil moisture data compiled from 8 stations in iRON.

iRON 1 was installed in 2012, and iRON 8 was installed in 2016. Each station collects volumetric soil water content (VWC) data (m^3 / m^3) from a 20 cm soil depth, at 20-minute intervals. VWC is simply the ratio of the volume of water to the unit volume of soil (Datta et al., 2018). Collectively, this investigation utilized several million discrete soil moisture measurements. For a comprehensive outlook on seasonal soil moisture variability throughout the Roaring Fork Watershed, monthly-averaged volumetric soil moisture was estimated.

Soil moisture throughout the watershed for all twelve months was interpolated using ArcGIS Pro's Inverse Distance Weighting (IDW) interpolation method. IDW interpolation was implemented to minimize distal interpretation of soil moisture values since the majority of iRON stations are confined to the Roaring Fork Valley. The seasonal variability of soil moisture is most apparent in January, May, and August. The soil moisture regime exhibits peak soil water storage in August, as seen in Figure 4. In August, VWC near the confluence of the Roaring Fork and Fryingpan Rivers is about 70%. The occurrence of peak soil moisture in August is likely related to the timing of the North American Monsoon, which begins in July and persists through late August (Colorado Climate Center, 2023).
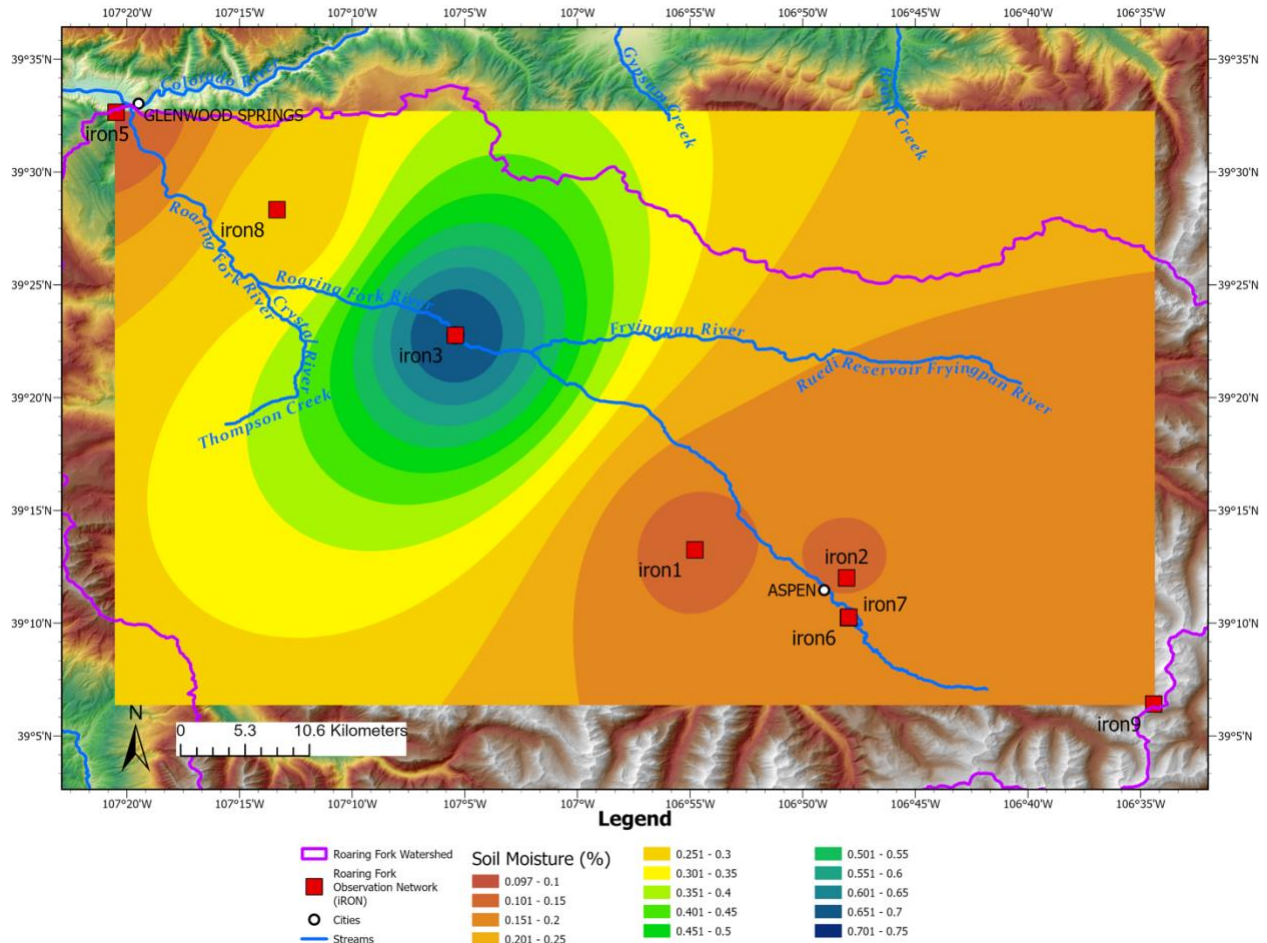
Figure 4. Interpolated volumetric soil water content for August. The soil moisture regime exhibits peak soil water storage in August, with a VWC of 0.7 – 0.75 at the confluence of the Roaring Fork River and Frying Pan River.

Figure 6 shows minimum soil water storage in May and Figure 6 shows intermediate conditions in January. Again, peak soil water storage is at the confluence of the Roaring Fork and Fryingpan Rivers.
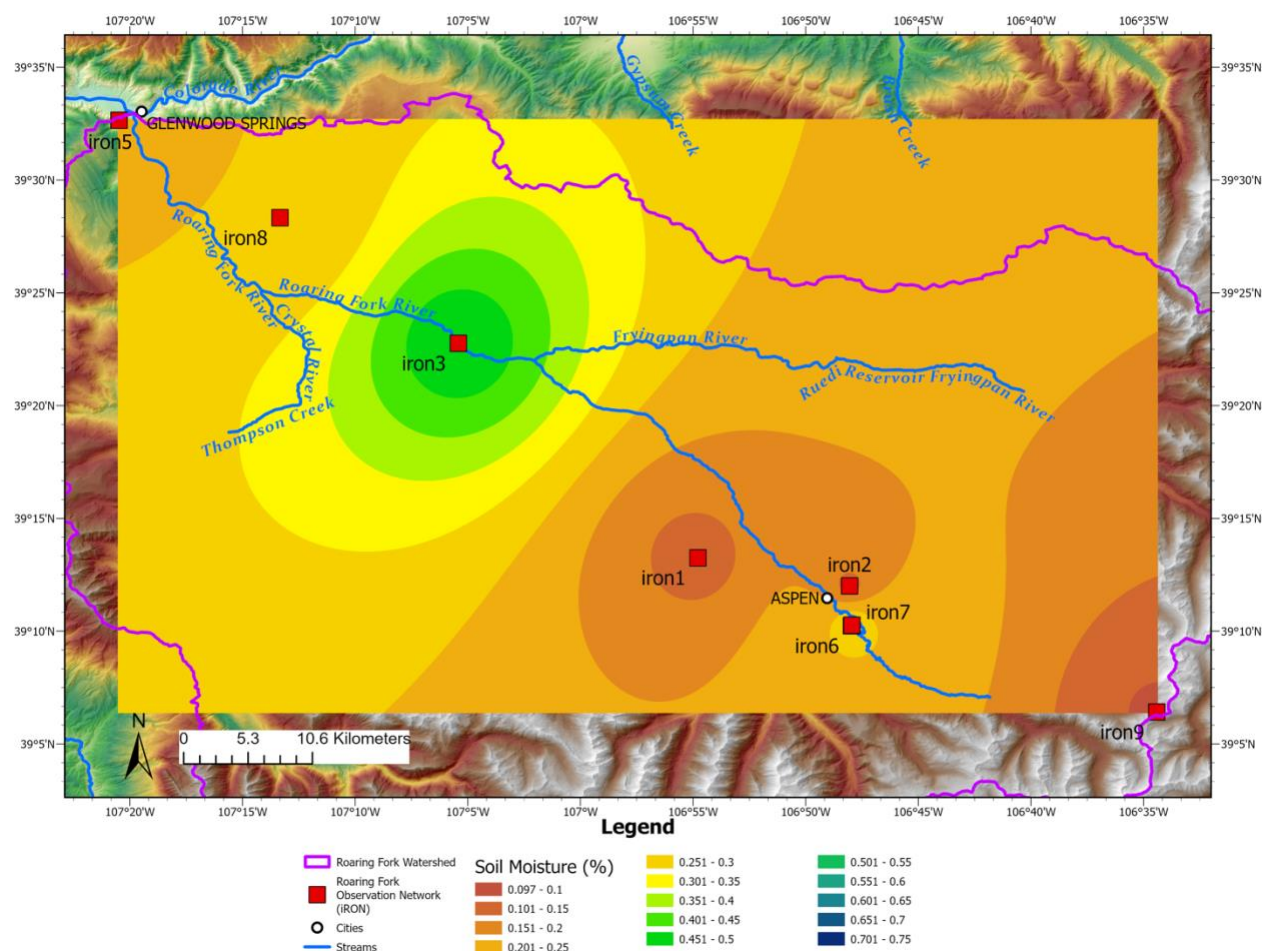
Figure 5. Interpolated volumetric soil water content (VWC) for January. VWC is the ratio of the volume of water to the unit volume of soil. Soil moisture ranges vastly in the watershed with a range of 1 to 75%. Soil water content is perpetually highest near the confluence of the Roaring Fork River and Fryingpan River. In January, the peak VWC is between 0.45 and 0.5 (45 to 50%) (Aspen Global Change Institute, 2023).
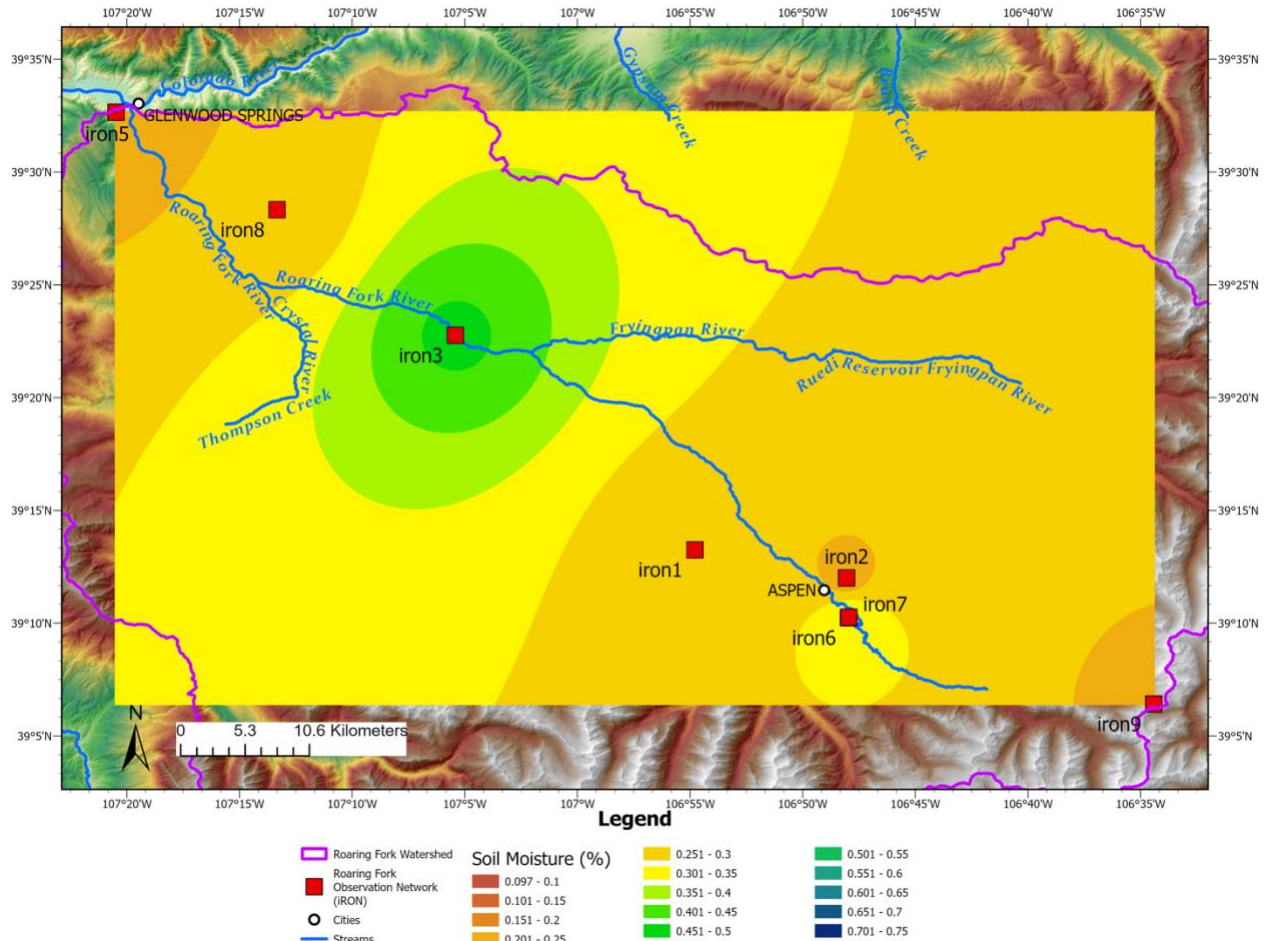
Figure 6. Interpolated volumetric soil water content for May. Soil water content is lowest in May. Peak VWC in May is between 0.45 and 0.5.

As the inception of iRON is related to monitoring climate change dynamics, the University of California Merced's Climate Toolbox was utilized to estimate the Roaring Fork watershed's response to a Representative Concentration Pathway (RCP) 8.5 emissions scenario (UC Merced Climate Toolbox, 2023). Projections are based on the USGS' monthly water balance model (MWBMM) (Bock, 2016). As described by the Intergovernmental Panel on Climate Change (IPCC), the RCP 8.5 emissions scenario is the highest baseline emissions scenario in which emissions continue to rise throughout the 21st century (IPCC, 2013). This emissions scenario produces a substantial increase in evapotranspiration (ET) and a decrease in estimated soil

moisture availability in the fall months, depicted in Figure 7. Both of these may have

implications for baseflow, which accounts for virtually all streamflow in these months.
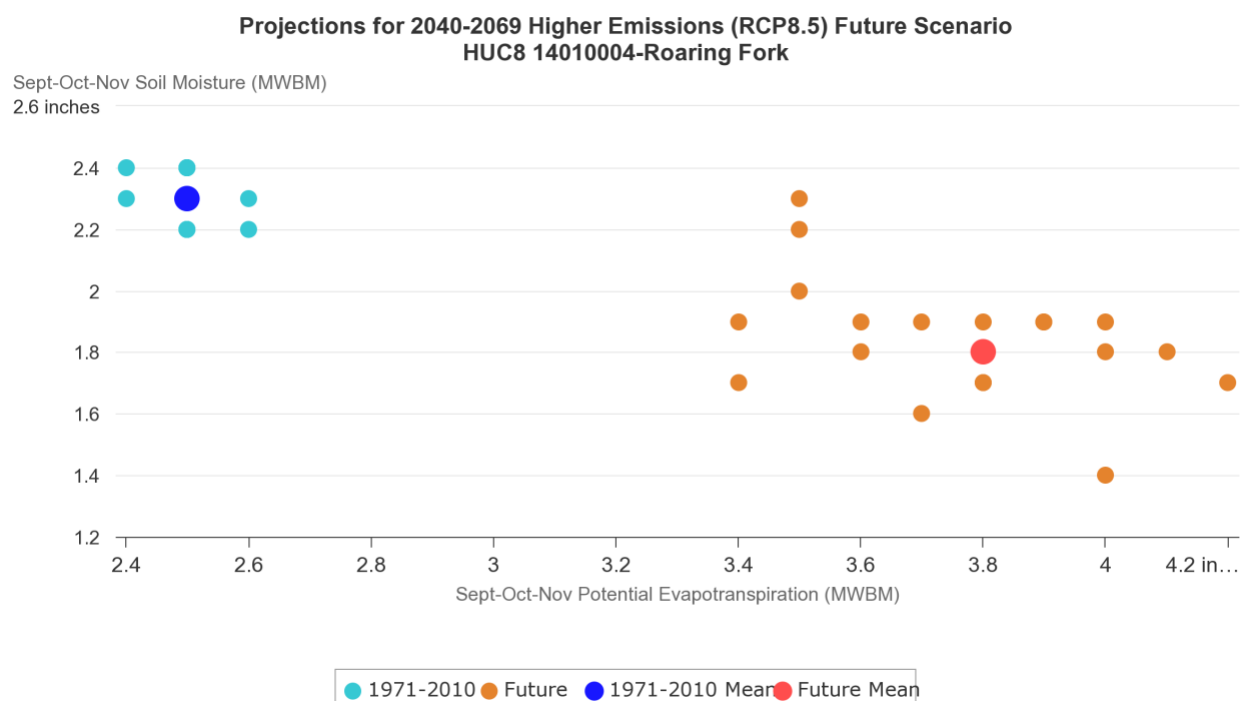
Figure 7. Projected soil moisture response to climate variability in the Roaring Fork Watershed. In an RCP 8.5 emissions scenario, there is a pronounced effect on potential evapotranspiration (PET, in.) and soil water storage (SOIL, in.). In the Roaring Fork Watershed, there will be significantly higher PET, resulting in less SOIL. Projections are derived from the USGS Monthly Water Balance Model Futures (UC Merced Climate Toolbox, 2023).

Hewlett (1961) proposed the concept of soil moisture flux as a source of baseflow in steep

mountain watersheds and suggested the possibility of unsaturated flow, where drainage is a

product of tension, rather than positive hydraulic gradients. This study constructed a physical

hillslope model at the Coweeta Hydrologic Laboratory, with an unsaturated soil moisture profile,

and observed vertical and slope-wide gradients in soil moisture tension, with more water

retention downslope than upslope. This considered, it is feasible that vadose soil moisture flux

may have some role in baseflow contribution in forested areas with a thick soil mantle. Peak soil

water storage in the Roaring Fork Watershed aligns both spatially and temporally with peak

baseflow contribution, with a VWC of more than 70% at the confluence of the Roaring Fork and

Fryingpan Rivers in August.

  d. Roaring Fork River Flow Regime

The Roaring Fork River exhibits a flow regime consistent with other snowmelt-fed systems.

Figure 8 shows that for the USGS gauge "Roaring Fork River near Aspen, CO", peak discharge

is on the order of 200 ft^3 / s (5.66 m^3 / s) in May, deriving from snowmelt runoff. Baseflow

conditions persist from July to March, with a discharge of less than 50 ft^3 / s (1.42 m^3 / s)
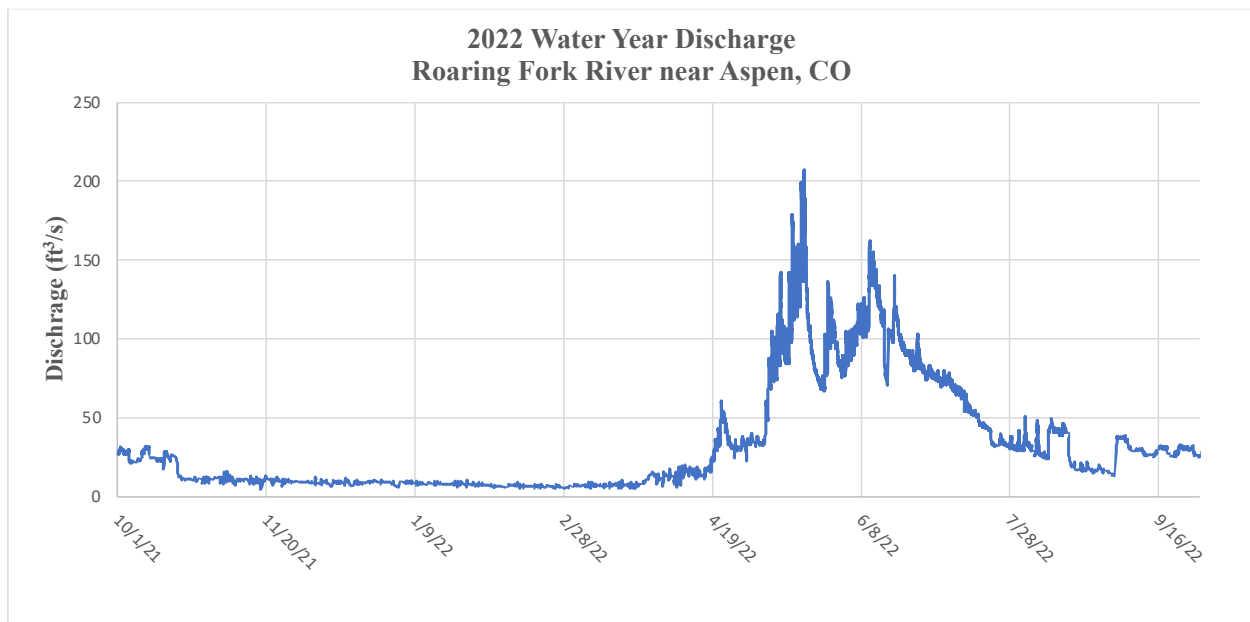
Figure 8. 2022 Water Year Hydrograph of the Roaring Fork River near Aspen, CO. A peak discharge of 200 ft3/s occurs in May, while baseflow conditions persist from August to March. The 2022 water year is a low-flow year (USGS National Water Information System, 2023).

Figure 9, a raster hydrograph, visualizes inter-annual and intra-annual variations in

streamflow. Days of the year are depicted on the x-axis, and years are depicted on the y-axis.

Therefore, the gradated color of each pixel visualizes stream discharge for any given day from

1984 - 2023. The raster hydrograph confirms the snowmelt regime with peak discharges in May

and highlights enigmatic water years. For instance, in 1995 and 2019, there was a significant lag

time in peak discharge. In most years, discharge surpasses $400 +$ ft^3 /s (11.33 m^3/s). The raster

hydrograph emphasizes that low flow, or baseflow conditions, persist from August to March. The

persistence of low-flow, or baseflow, conditions, and the brief duration of snowmelt runoff

provide preliminary insight into the large and stable groundwater contribution received by the

Roaring Fork River. At the Roaring Fork River near Aspen stream gauge, a discharge of 100 ft^3

/s is only equaled or exceeded 20% of the time, which is a response to overland flow derived

from snowmelt and implies that the stream is largely supported by groundwater contribution for

the remainder of the year.
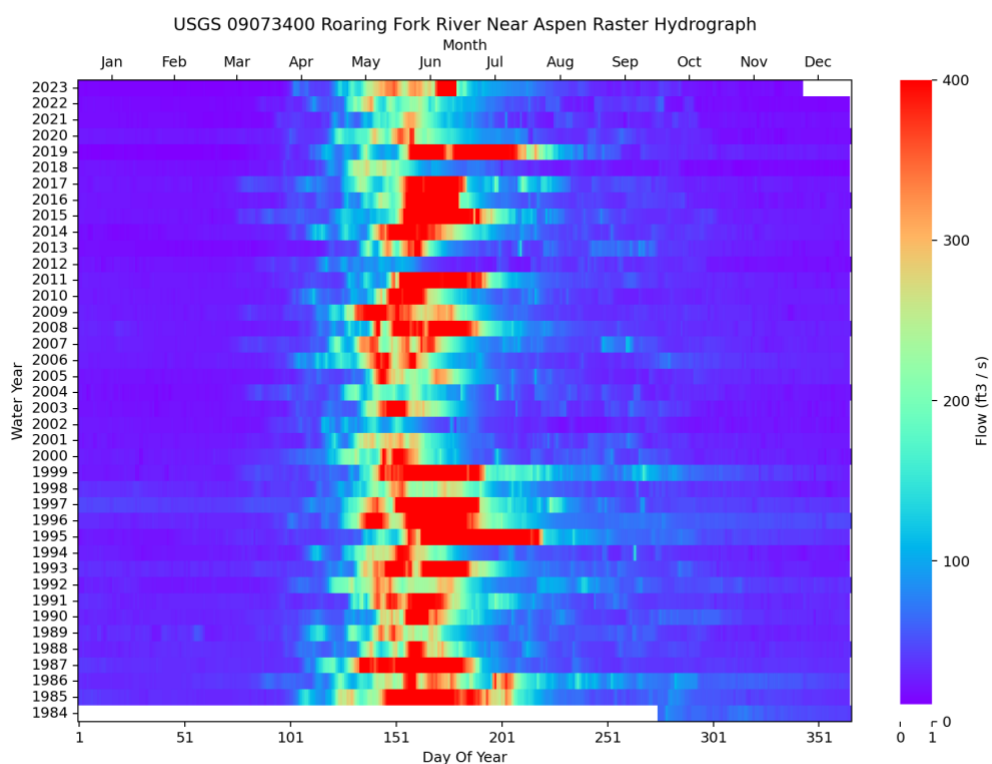
Figure 9. Raster hydrograph of the Roaring Fork River near Aspen, CO. This raster visualizes
daily discharge at USGS site Roaring Fork River near Aspen, CO for 1984 – 2023. The flow
regime is characterized by a peak discharge in late May / early June and baseflow conditions in

August through March. The hydrograph does not exhibit any patterns of anthropogenic flow alteration. (USGS National Water Information System, 2023).

III.   QUANTIFYING BASEFLOW USING GROUNDWATER LEVELS

a. <u>Data Sources and Data Editing</u>

The CDWR operates a well-permitting database that contains hydrographic data for every permitted well in the state of Colorado. Within the graphical user interface, which contains a generic search tool and an interactive map search tool, users may specify parameters such as geographic location, permit status, and permitted use to produce an inquiry that populates the map with all corresponding well permits. Figure 10 shows an example inquiry for all wells in Pitkin County, comprising most of the Roaring Fork Watershed. Comparable datasets can be retrieved from any respective state's Department of Natural Resources or the USGS National Groundwater Monitoring Network.
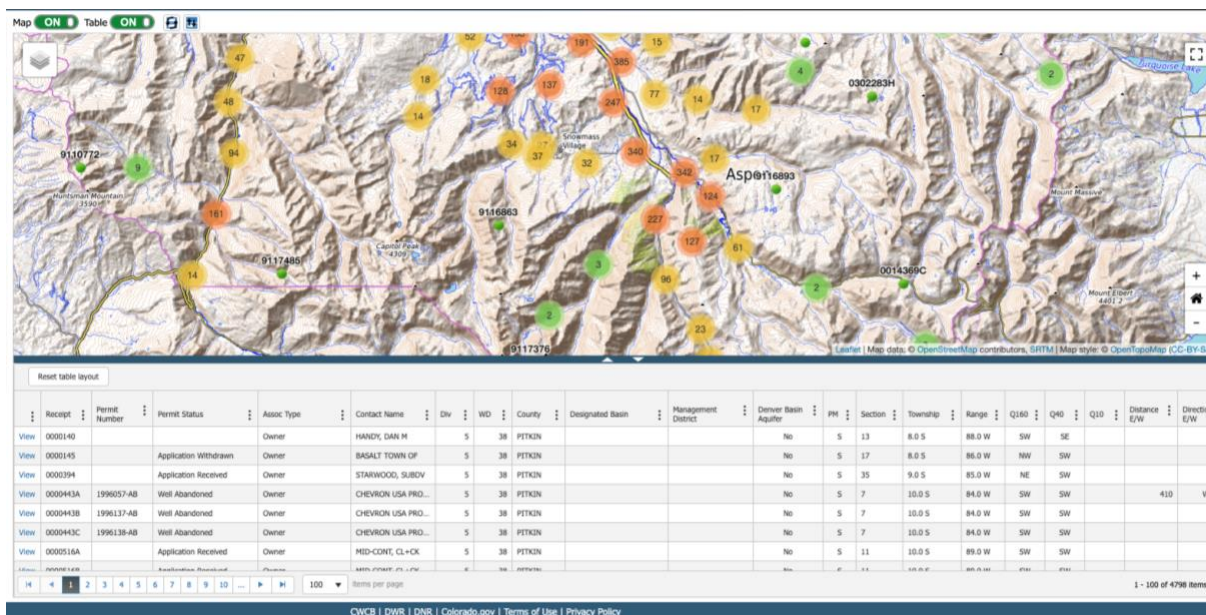
Figure 10. Colorado Division of Water Resources well permit search tool. In this map view, an inquiry of all well permits in Pitkin County was entered. This yields data for 4,782 wells. Available at: https://dwr.state.co.us/Tools/WellPermits (Last accessed: March 2024).

The CDWR well-permitting database readily allows users to export this data as a spreadsheet (.csv file), which contains a variety of relevant parameters. The parameters most pertinent to this investigation are well coordinates, construction date, elevation, completed well depth, and static water level. Furthermore, the outputted tabular data contains an embedded link for each well leading to an imaged document of the physical well permit, sometimes containing pumping test data. Generally, wells with pumping test data contained a well log. From well logs, an average thickness of 40 m was gleaned for the Roaring Fork alluvial aquifer.

To prepare the data for groundwater level interpolation, static water level measurements, which are observed depth-to-water measurements, were subtracted from the land surface elevation, yielding a groundwater surface elevation. In the preliminary analysis of the groundwater level data, it was discerned that measurements before 2000 were comparatively sparse and had a higher frequency of outlying measurements. To limit the effect of temporal oscillations in groundwater levels, and better constrain an estimate of present groundwater conditions, a reduced period from 2000 to 2022 was selected. Since most pumping tests were conducted in the alluvial aquifer, an alluvial aquifer dataset was partitioned, selecting only wells shallower than 40 m. The shallow subset contains estimated groundwater levels from 151 wells.

Finally, the data from 58 pumping tests were manually compiled into a spreadsheet. Municipal wells are confined within the Roaring Fork Valley, as this is the region's most dense populous. The data from the 58 pumping test wells include the static water level before the test, test duration, sustained yield, and final water level.

Other mapped features were collected from a variety of USGS online databases. Stream gauge locations were sourced from the USGS National Water Information System (NWIS) (http://waterdata.usgs.gov/nwis). Shapefiles for streams were collected from the USGS National

Hydrography Dataset (NHD) (https://www.usgs.gov/national-hydrography/national-hydrography-dataset). Finally, the watershed boundary was downloaded from the USGS Watershed Boundary Dataset (WBD) (https://www.usgs.gov/national-hydrography/watershed-boundary-dataset). The drainage of the Roaring Fork River is classified by the USGS as a subbasin and is therefore contained within the Hydrologic Unit 8 dataset.

b. Groundwater Level Interpolation

A map of groundwater surface elevation was created in ArcGIS Pro by interpolating the static groundwater levels. Bayesian empirical kriging, inverse distance weighted (IDW), and natural neighbor interpolation methods were all tested, but the natural neighbor method was implemented since it abstains from producing peaks, ridges, and valleys that are not represented by the input samples (Sibson, 1981). Natural neighbor interpolation was conducted for the superset and the alluvial aquifer subset. The outputted raster was then visualized using the contouring tool and overlayed on the topography. The point feature of each well also symbolizes well depth with graduated colors.

Groundwater level contours were used to estimate hydraulic gradient ($\frac{dh}{dl}$), a measure of the change in hydraulic head, with distance. Hydraulic head (h) is the mechanical energy per unit weight of water and is easily represented by a water level elevation in a well (Fetter and Kreamer, 2021). To estimate hydraulic gradient, one must discern the change in hydraulic head between two points over a known transect length between these points. Groundwater flow is in the direction of decreasing hydraulic head (Fetter and Kreamer, 2021). Thus, by measuring the distance between two contours of a known hydraulic head, the hydraulic gradient, a vector, is estimated. These measurements inform the direction of groundwater flow within the system. Transects for hydraulic gradient, which glean flow paths, were drawn throughout the watershed

and measured using ArcGIS' native measuring tool. Flow paths are drawn orthogonally to the groundwater surface.

c. Assessment of Hydraulic Conductivity of the Roaring Fork alluvial aquifer

This study utilized established empirical pumping test formulae on pumping test data from 57 wells to establish a hydraulic conductivity for the study. The spatial distribution of pumping tests is mostly confined to the Roaring Fork Valley near the town of Aspen, as this is the only largely populated region within the watershed. Thus, the assessment of hydraulic conductivity does not necessarily inform hydraulic properties for the rest of the watershed.

The specific capacity (S_c) of a well is established by dividing the yield of the well by the drawdown (Fetter and Kreamer, 2021):

$$S_c = \frac{Q}{s} \qquad (1)$$

where Q is the yield of the well (L^3/T) and s is the drawdown (L). In this case, specific capacity (S_c) has units of gpm/ft.

Transmissivity (T, L^2/T), a measure of the amount of water that can be transmitted horizontally through a unit width of the entire saturated thickness of an aquifer, is estimated by a relationship established by Driscoll (1986):

$$T = 1500 \times S_c \qquad (2)$$

Hydraulic conductivity (K, L/T), a controlling factor for groundwater flow, describes a system's ability to transmit fluid (Fetter and Kreamer, 2021). It is estimated with:

$$K = \frac{T}{b} \qquad\qquad (3)$$

where b (L) is the saturated thickness of the alluvial aquifer.

This series of calculations were conducted for 58 wells to find the average hydraulic conductivity of the alluvial aquifer. A complete table of hydraulic conductivity estimates is seen in Appendix A.

d. Estimating Groundwater Discharge to the Roaring Fork River

Groundwater discharge (Q, L^3/T) to the Roaring Fork River was estimated to ultimately establish a baseflow index (BFI, [1]), the ratio of mean annual baseflow to mean annual streamflow. Darcy's law, an empirical formula, states that the discharge of water (Q) through a unit area of a porous medium is proportional to the hydraulic gradient ($\frac{dh}{dl}$), hydraulic conductivity (K), and area (A) that is normal to the hydraulic gradient (Fetter and Kreamer, 2021):

$$Q = -KA\frac{dh}{dl} \qquad\qquad (4)$$

Calculating a cross-sectional aquifer area (A) perpendicular to the stream requires an estimate of both the aquifer thickness (b) and length (l). Observations from a field reconnaissance were used to inform an estimate of the length of the aquifer, where it was gleaned that much of the upstream channel is incised bedrock. The alluvial aquifer, which is substantially more prolific than the bedrock aquifer, is considered to account for the bulk of groundwater discharge to the Roaring Fork River. Streams draining steep mountainous terrain, like the Roaring Fork River, generally have a higher percentage of shallow groundwater signatures, where most of the groundwater contribution occurs at depths less than 6 m (Hare et al., 2021). On the basis of averaged hydraulic gradient and hydraulic conductivity, a groundwater discharge

to the Roaring Fork River is estimated with Darcy's law. Since groundwater discharge to a

stream is bilateral, the estimated groundwater discharge must be increased by a factor of 2.

Finally, the mean annual groundwater discharge is divided by the mean annual streamflow to

establish a BFI for the Roaring Fork River.

IV.   GRAPHICAL BASEFLOW ANALYSIS

Traditional analysis of baseflow was conducted using Eckhardt's recursive digital filter, a

method of hydrograph separation, in version 1.1 of the USGS' Hydrologic Toolbox software

package. Eckhardt's recursive digital filter is described by the equation below:

$$b_k = \frac{(1-BFI_{max})ab_{k-1}+(1-a)BFI_{max}y_k}{1-aBFI_{max}} \qquad (5)$$

Where b is the baseflow, y is the streamflow, k is the time step number, and a and BFI_{max} are

parameters whose values must be set before applying the filter (Eckhardt, 2005). BFI_{max} is

estimated by a priori-defined value according to the hydrologic and hydrogeologic characteristics

of the basin (Collischonn and Fan, 2012). The Roaring Fork River is characterized as a perennial

stream with a porous aquifer and has a representative $BFI_{max} = 0.8$. The USGS Hydrologic

Toolbox is a graphical user interface that is embedded with hydrologic data from the NWIS and

therefore automates much of the process for running a recursive digital filter. For the purpose of

this study, default filter parameters were used for an upstream gauge and a downstream gauge:

Roaring Fork River near Aspen and Roaring Fork River at Glenwood Springs. These gages are

located in the watershed's two principal townships: Aspen and Glenwood Springs. To compare

Eckhardt's recursive digital filter to other available hydrograph separation methods, a

hydrograph separation was also conducted using all other available methods in the USGS

Hydrologic Toolbox.

V.   RESULTS AND DISCUSSION

Groundwater Levels and Hydraulic Gradients

Figure 11 shows groundwater levels interpolated from the shallow well subset via the natural neighbor geoprocessing tool, with flow paths representative of $\frac{dh}{dl}$ estimates. The groundwater level map from the superset of wells is presented in Figure 12. On this map, the completed well depths range from 2 to 300 meters. In comparison, this map manifests a more complex groundwater surface, with more peaks and ridges. At distal regions of both contour maps, hydraulic gradients are noticeably steeper, which is a product of boundary assumptions of the contouring tool, rather than true hydrogeologic conditions. Groundwater levels within the basin range from about 2000 to 2850 meters above mean sea level, with groundwater levels lowest proximal to the Roaring Fork River. The perched water table seen south of Aspen corresponds to the Aspen Mountain Syncline. The perched water table likely derives from groundwater migrating through the uppermost layer of the syncline, the Belden Formation (Pb), and then being trapped by the underlying impervious aplite porphyry (TKap).
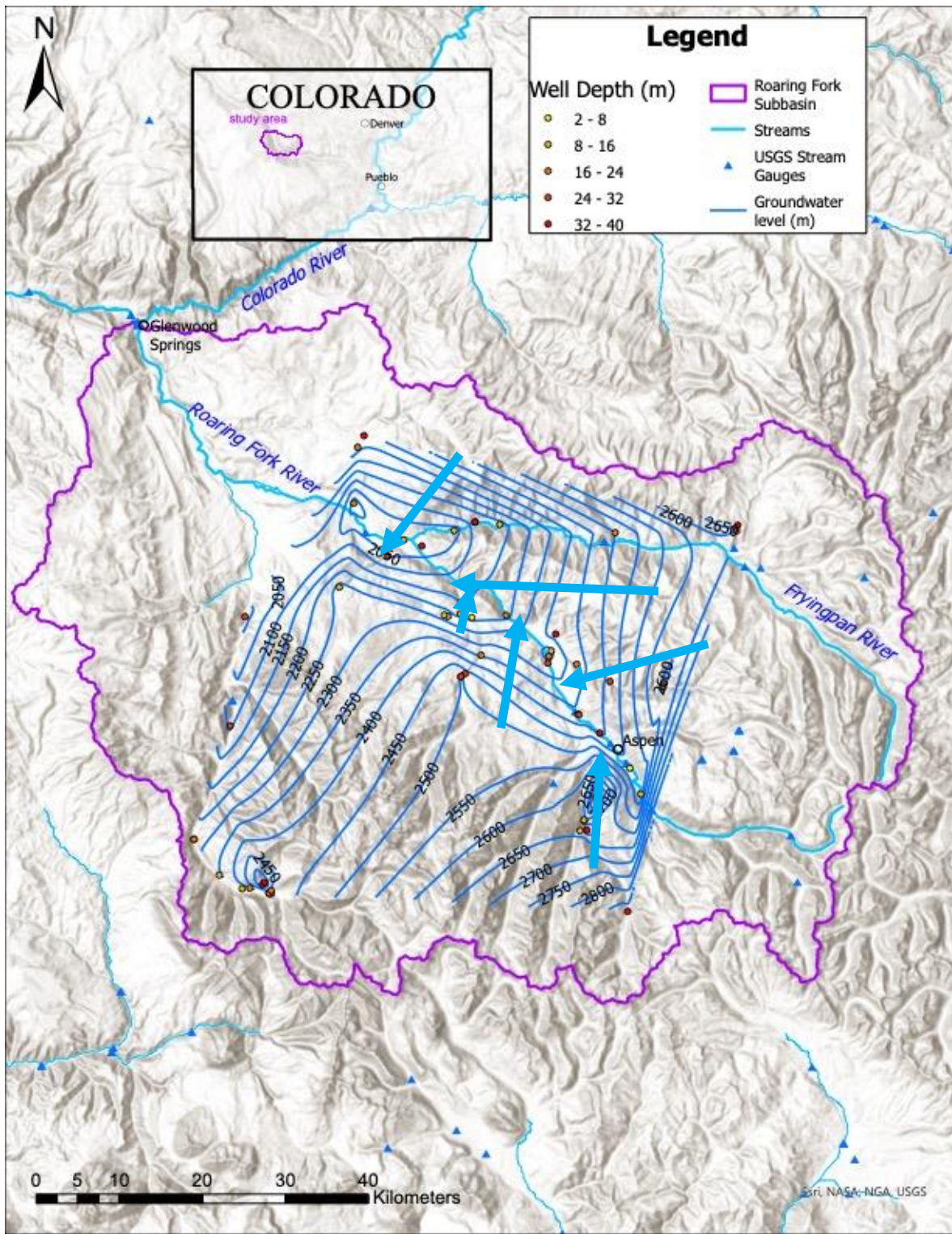
Figure 11. Interpolated groundwater levels from the shallow wells subset. The groundwater levels (blue) is overlying topography, with representative flow paths shown (blue arrow). Gradated circles represent completed well depth in meters.
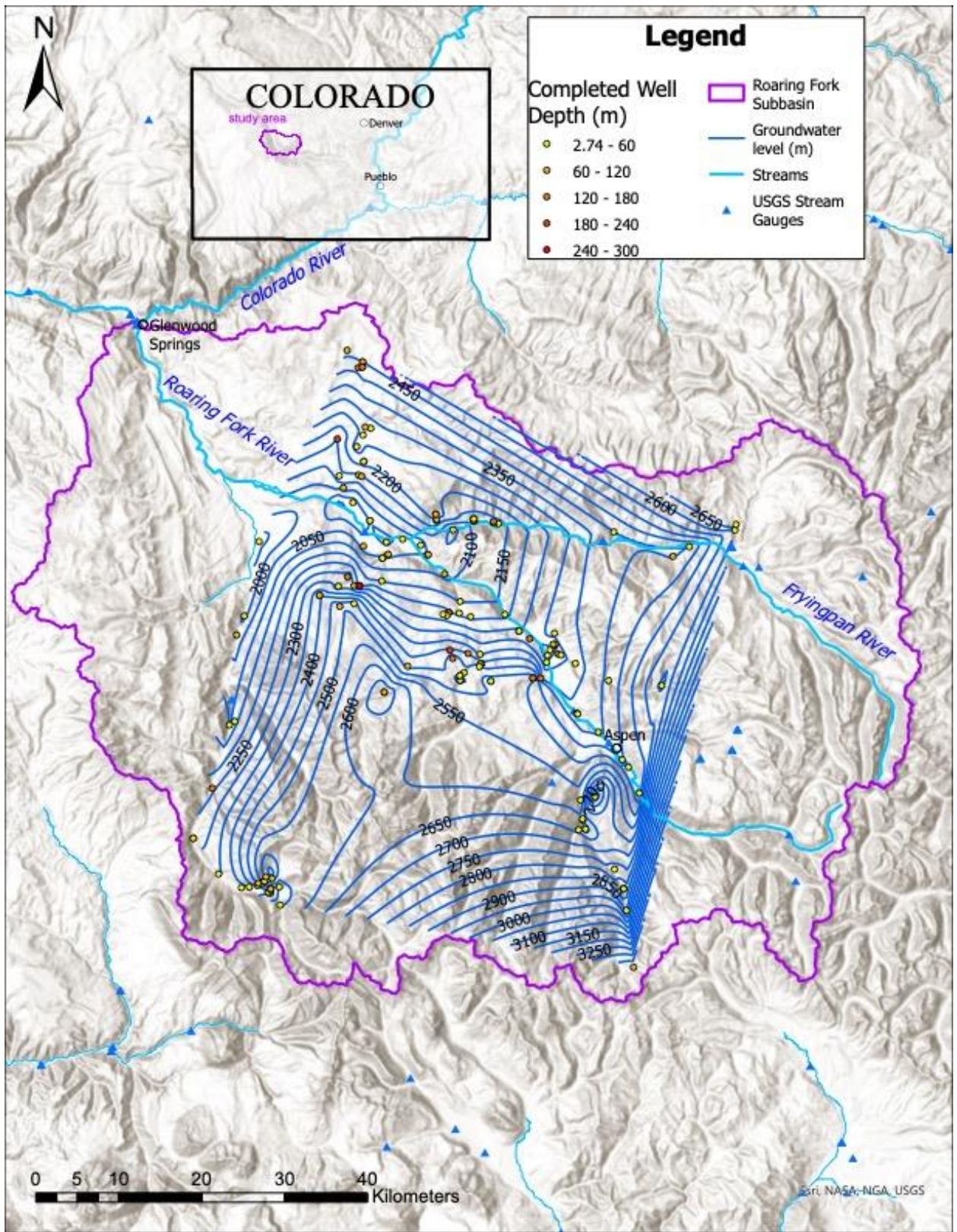
Figure 12. Interpolated groundwater levels for all wells.

The results for hydraulic gradients ($\frac{dh}{dl}$) estimated via discernible flow paths in the interpolated groundwater level map are summarized in Table 5.1. The average hydraulic gradient was 0.023 [1]. All calculations were made using the shallow wells subset, as it better represents the shallow groundwater signature for the basin. Tables including hydraulic gradients across all interpolation methods are included in Appendix B, along with hydraulic gradients estimated for the superset of groundwater level data.

Table 1. Estimated hydraulic gradients

Horizontal Transect Distance (m)	Change in Groundwater Level (m)	Hydraulic Gradient
14000	400	0.029
40000	600	0.015
15200	275	0.018
11300	350	0.031
9300	300	0.032
8160	100	0.012

Hydraulic Conductivity

The average hydraulic conductivity (K) for the Roaring Fork alluvial aquifer estimated by Driscoll's (1986) empirical formulae is 1.46 x 10^{-3} m / s, which is typical for that of a gravelly alluvial aquifer. A table including all of the intermediate calculations for specific capacity (S_c) and transmissivity (T), as well as estimated hydraulic conductivities (K), is included in Appendix C.

Groundwater Discharge

An average groundwater discharge of 1.57 m^3 / s is quantified for the Roaring Fork River, at the Aspen stream gauge, using Darcy's law. The Roaring Fork River near Aspen stream gauge

is employed as the gauge of interest, as this is where hydrogeologic parameters are best informed. Average values for hydraulic conductivity and hydraulic gradient were used alongside an estimate of the cross-sectional area of the alluvial aquifer. For the cross-sectional area, an aquifer thickness (b) of 6 m was used, representative of a shallow groundwater signature, which is characteristic of drainages in steep mountainous terrain (Hare et al., 2021). For length (l), a horizontal transect length of about 3,900 m was measured in ArcGIS Pro. The horizontal transect length begins at the gauge of interest and measures only the segment of the longitudinal stream profile that incises alluvium, terminating at the bedrock-incised channel. The longitudinal change from bedrock to alluvial substrate is apparent via a distinct change in declivity adjacent to the stream. To estimate the BFI, the USGS StreamStats gauging profile for the Roaring Fork River near Aspen gauge was used to constrain a mean annual streamflow of 2.75 m^3 / s (USGS, 2023). This discharge accounts for a substantial BFI of 0.57 for the Roaring Fork River near the Aspen gauge location, implying that 57% of streamflow derives from groundwater.

Hydrograph Separation

As the efficacy of a given hydrograph method may vary with watershed characteristics, a first-order hydrograph separation was conducted with all methods, as seen in Figure 13. Eckhardt's method is denoted on the graph as "Two PRDF", or two-parameter differential filter. In comparison, Eckhardt's filter is a more liberal estimate of baseflow for this study, yielding a BFI of 0.72. Most methods of hydrograph separation convey similar baseflow indices, excluding the BFI standard and BFI modified methods, which exhibit more conservative estimates of baseflow.
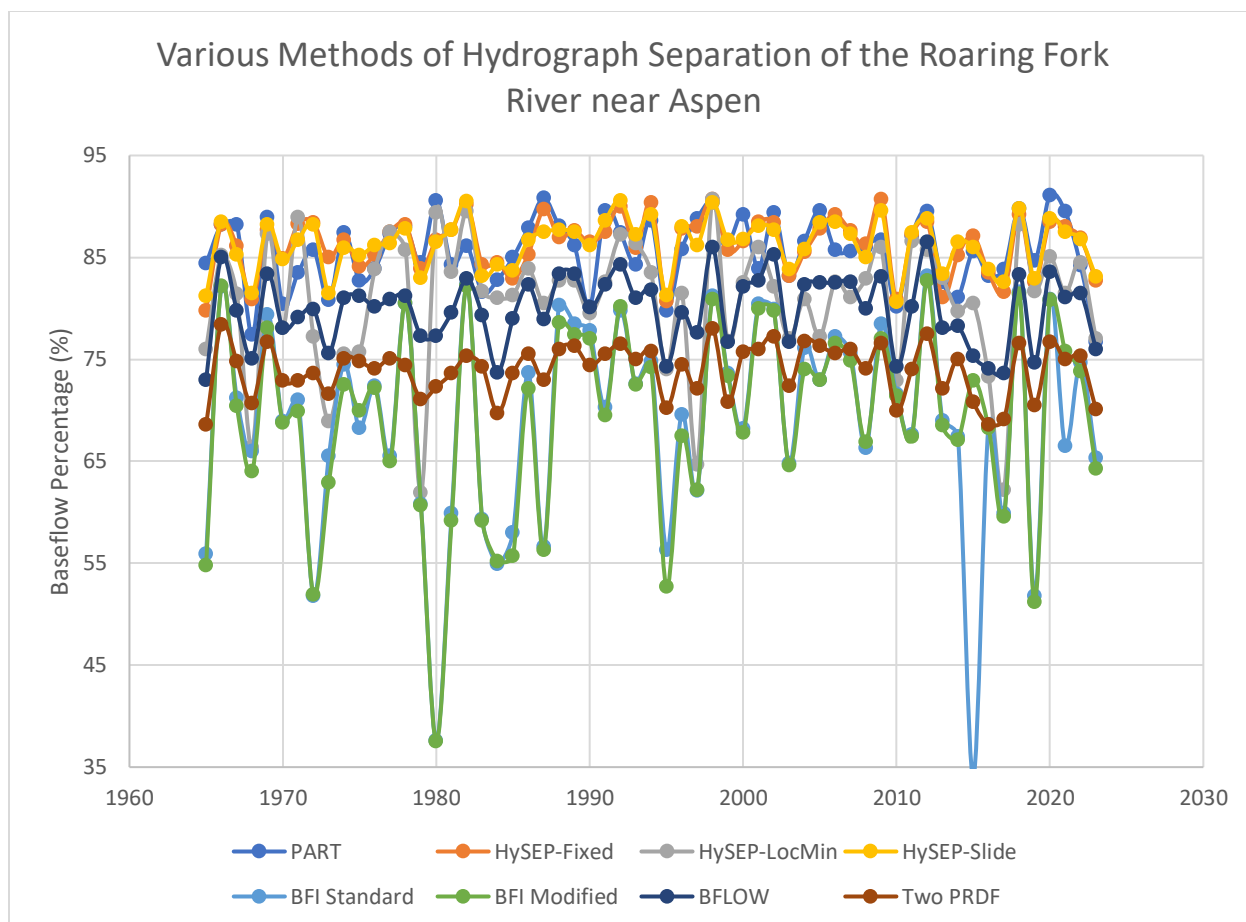
Figure 13. Hydrograph separation methods available in USGS Hydrologic Toolbox 1.1 and comparative baseflow percentage estimates. The most conservative estimates of baseflow are yielded by the modified BFI method, while the sliding interval hydrograph separation yields the highest baseflow estimate (USGS, 2024).

The hydrograph separation conducted on the downstream gauge; the Roaring Fork River at Glenwood Springs is seen in Figure 14. This displays the mean annual baseflow in comparison to the mean annual streamflow and estimated runoff, for each year on the operational record. Annual precipitation data is plotted on the secondary axis (City of Aspen Water Department, 2023). Intuitively, years of high precipitation correspond to years of high baseflow and streamflow. Since baseflow contribution in the watershed is dominated by shallow, near-stream, low residence time subsurface flow, any groundwater recharge that occurs will likely reach the stream with transit times on the order of weeks to years (Miller et al., 2014).
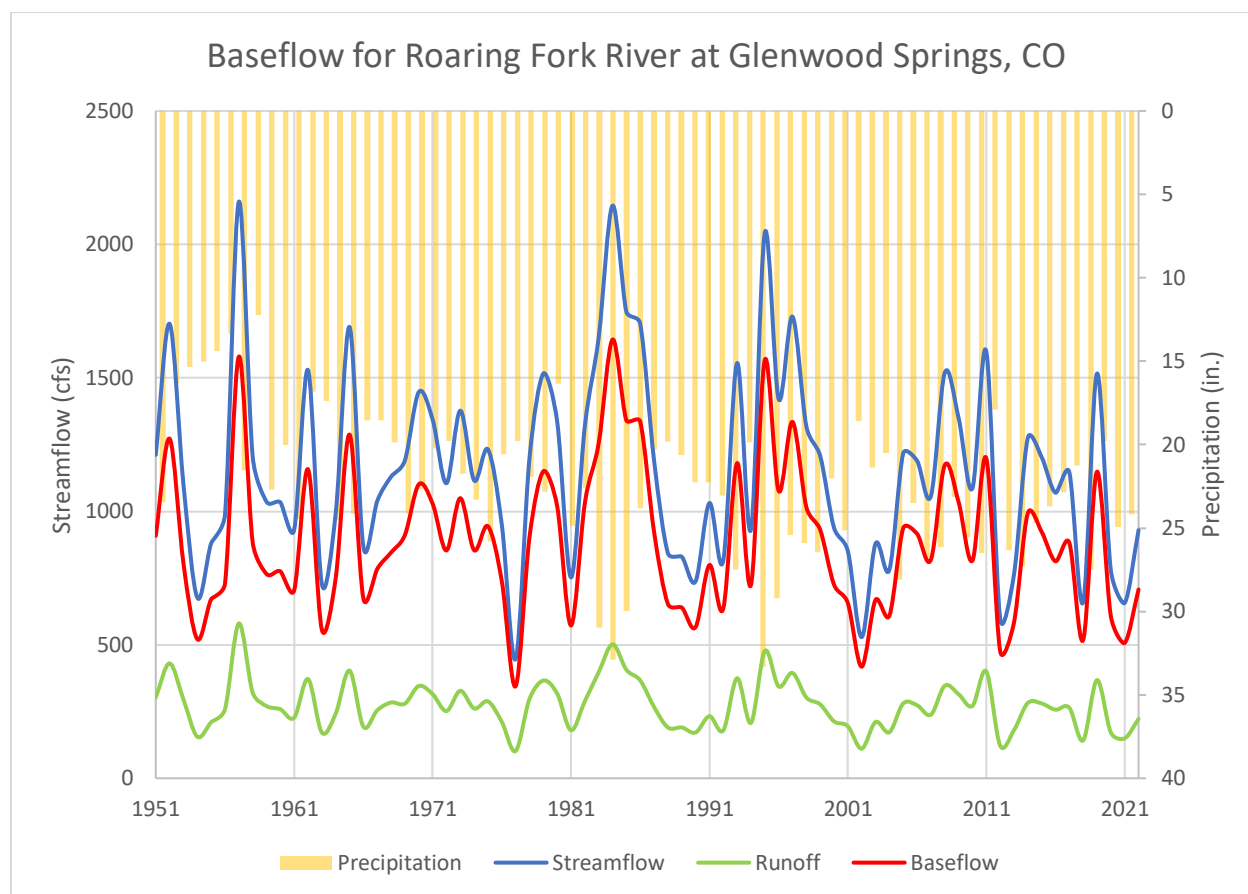
Figure 14. Eckhardt's recursive digital filter for the Roaring Fork River near Glenwood Springs, CO, with precipitation data (City of Aspen Water Department, 2023). The red line, partitioned baseflow, shows that baseflow accounts for most of the streamflow (USGS, 2024).

For the upstream gauge, the Roaring Fork River near Aspen, the hydrograph separation is seen in

Figure 15. This appears to follow a similar pattern of baseflow contribution, where most of the

streamflow is accounted for by baseflow.
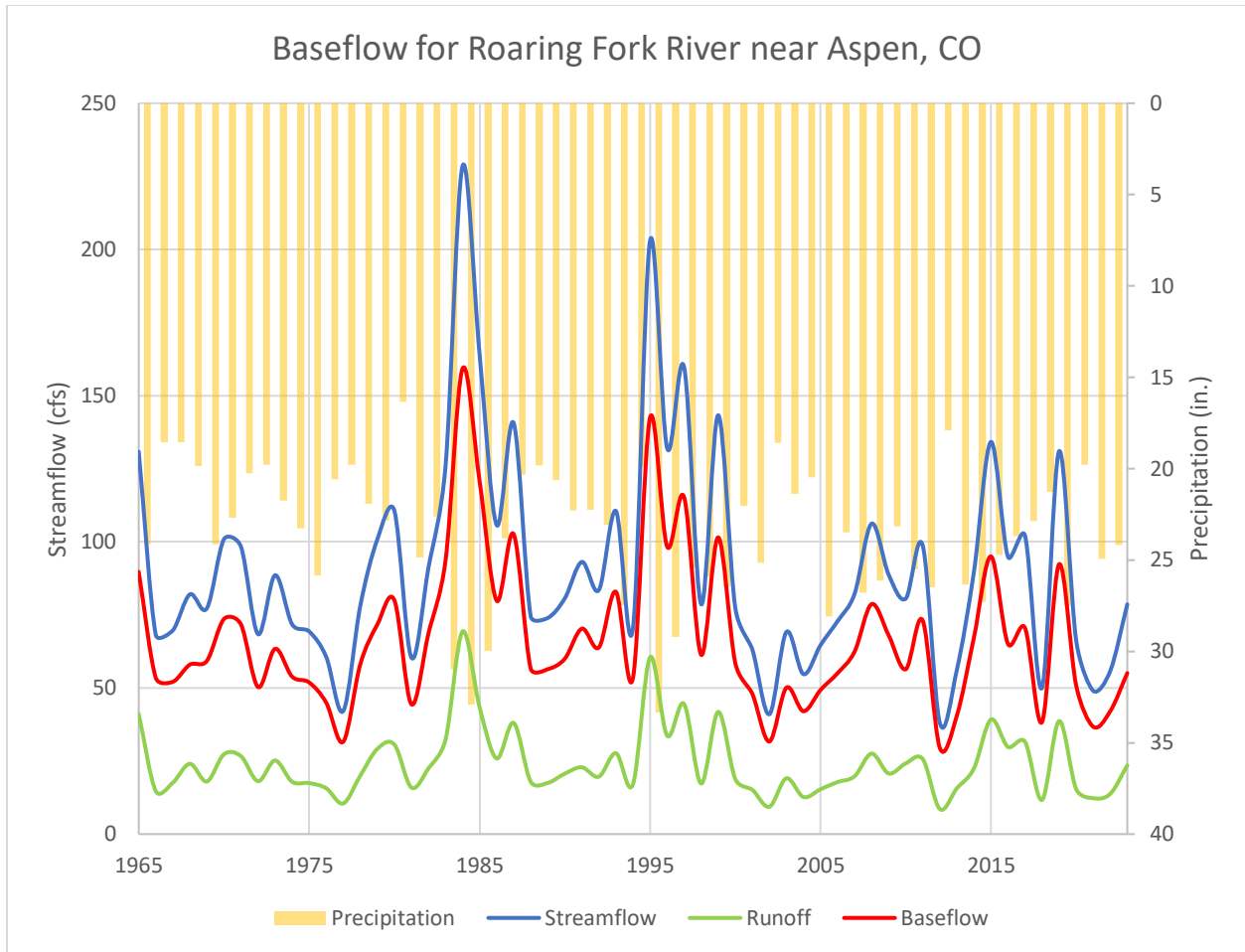
Figure 15. Eckhardt's recursive digital filter for the Roaring Fork River near Aspen, CO, with precipitation data (City of Aspen Water Department, USGS).

Figure 16 compares seasonal oscillations in BFI between the Aspen and Glenwood Springs gauge locations. Although these gauges constitute a significant change in elevation, stream discharge, and hydrology, they mostly account for similar BFIs throughout the year. The largest deviation in BFI occurs in August when the BFI for the downstream location (Glenwood Springs) is about 0.11(11%) more than that of the upstream location (Aspen).
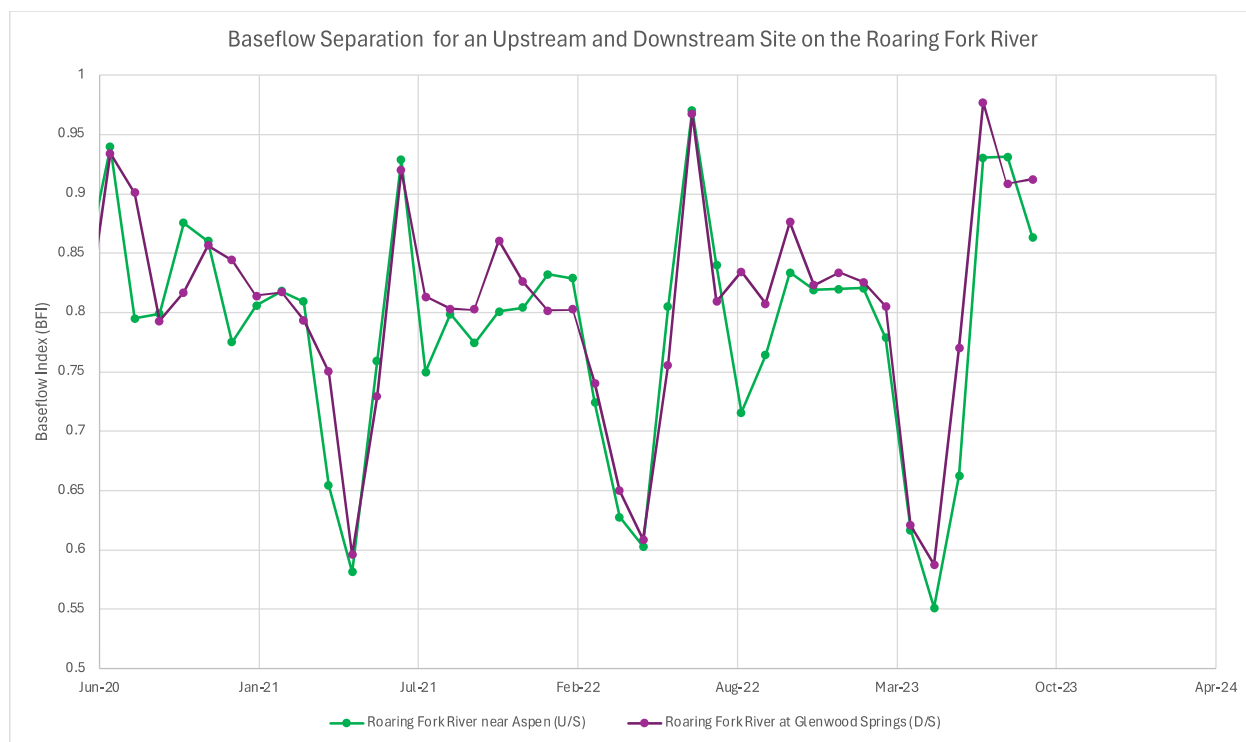
Figure 16. Comparing Baseflow Indices between an upstream and downstream site on the Roaring Fork River (USGS, 2024).

VI.   CONCLUSIONS

On the basis of averaged hydraulic conductivities and hydraulic gradients established from over 150 well permits within the Roaring Fork Watershed, a baseflow yield and BFI were determined for the Roaring Fork River. This study substantiates groundwaters' imperative role in sustaining streamflow, where it is elucidated that, on average, 57% of streamflow in the Roaring Fork River originates as baseflow. Graphical methods of baseflow separation, such as Eckhardt's recursive digital filter, further establish groundwater's role in sustaining streamflow for high-elevation watersheds in the UCRB.

The results from this study have implications concerning comprehensive groundwater management practices in the UCRB. Climate change and anthropogenic activities such as groundwater pumping are likely to influence baseflow contributions in the UCRB (Miller et al.,

2014). Managing aquifer depletion near affluent streams, which may have proximal and distal consequences of depleting, or in some cases, causing cessation of streamflow, is imperative. Baseflow also plays an important role as a transport media for dissolved solids in the UCRB, where it is estimated that 89% of dissolved solids loads are delivered to streams via baseflow (Rumsey et al., 2017). Changes in baseflow may have pronounced effects on water chemistry in the UCRB, which may also constitute ecological effects. In light of overallocation issues and cutbacks in the UCRB, it is critical that studies as such inform future policymaking within the basin and that groundwater and surface water are recognized as a single, interconnected resource.

Publicly available groundwater data is a prudent method for quantifying baseflow contribution. As the national groundwater monitoring network expands, the efficacy of these methods will improve considerably. To date, no truly physically based methods are available to quantify baseflow. In hydrograph separation methods, the distinction between physically based and non-physically based methods is often made, but there are no in-situ measurements that directly relate to baseflow. Using publicly available groundwater data is cost-effective relative to other methods of quantifying baseflow, as it does not require costly instrumentation to measure parameters such as specific conductance (SC). This study, for the first time, demonstrates that publicly available groundwater level data can be utilized to supplement established methods of estimating baseflow. Enriching the arsenal of baseflow analyses will inform sustainable water resource management.

VII.   RECOMMENDATIONS

This study has limitations, such as uncertainties in the cross-sectional area of the alluvial aquifer and inaccuracies in hydraulic conductivity (K). Since there is a sparse history of hydrogeologic investigations in the watershed, assessing hydraulic conductivity (K) was

especially difficult and with uncertainties. The efficacy of the methods used in this study would benefit from a better assessment of the basin's hydrostratigraphy and hydraulic parameters of the alluvial aquifer. It would also benefit from a more expansive groundwater monitoring network within the watershed. It is recommended that the results from this study be compared with those of numerical groundwater models. Future research should consider investigating the interactions between groundwater pumping and baseflow contribution and perhaps conducting a specific conductance (SC) based hydrograph separation. Further investigating the ideas proposed by Hewlett (1961), and the implications of soil moisture flux as a source of baseflow in steep mountain watersheds is of special interest.

VIII. WORKS CITED

Anderson, R.S., Lehmann, B., Cusicanqui, D., Rossi, M.W. (2023). Climatic drivers of rock glacier dynamics: Mt Sopris Rock Glacier, CO, USA [poster abstract]. 2023 American Geophysical Union Meeting, San Francisco, CA, United States.

Barnes, B. S. (1939). The structure of base flow recession curves, *Trans. AGU*, **20**, 721–725, doi:10.1029/TR020i004p00721.

Bass, B., Goldenson, N., Rahimi, S., and Hall, A. (2023). Aridification of Colorado River Basin's Snowpack Regions Has Driven Water Losses Despite Ameliorating Effects of Vegetation: Water Resources Research, v. 59, doi:10.1029/2022wr033454.

Birkeland, P. W. (1973). Use of Relative Age-Dating Methods in a Stratigraphic Study of Rock Glacier Deposits, Mt. Sopris, Colorado. In Arctic and Alpine Research (Vol. 5, Issue 4, p. 401). Informa UK Limited. https://doi.org/10.2307/1550131

Bock, A. R., Hay, L. E., Markstrom, S. L., & Atkinson, R. D. (2016). Monthly Water Balance Model Hydrology Futures [dataset]. U.S. Geological Survey. https://doi.org/10.5066/F7VD6WJQ

Bryant, B., and Freeman, V.L. (1977). Geologic Summary of the Aspen Area, Southern Rocky Mountains, Colorado, *Rocky Mountain Association of Geologists*.

City of Aspen Water Department (2023). Aspen Colorado Precipitation Data, https://www.aspen.gov/DocumentCenter/View/500/Aspen-Precipitation-Data-Summary-1951---Present-PDF

Collischonn, W., & Fan, F. M. (2012). Defining parameters for Eckhardt's digital baseflow filter. In Hydrological Processes (Vol. 27, Issue 18, pp. 2614–2622). Wiley. https://doi.org/10.1002/hyp.9391

Colorado Climate Center (2023). North American Monsoon, *Colorado State University*, Fort Collins, CO.

Colorado Division of Water Resources (2023). Well Permits Search Tool: https://dwr.state.co.us/Tools/WellPermits

Datta, S., Taghvaeian, S., Stivers, J. (2018). Understanding Soil Water Content and Thresholds for Irrigation Management, *Oklahoma State University*.

Driscoll, F.G. (1986). Groundwater and Wells, 2nd edition, Johnson Division, St Paul, 1089

Eckhardt, K. (2005). How to construct recursive digital filters for baseflow separation, *Hydrol. Processes*, **19**, 507–515, doi:10.1002/hyp.5675.

Eckhardt, K. (2008). A comparison of baseflow indices, which were calculated with seven different baseflow separation methods, *J. Hydrol.*, **352**, 168–173, doi:10.1016/j.hydrol.2008.01.005.

Eckhardt, K. (2022). Technical note: Hydrograph separation: How physically based is recursive digital filtering? Copernicus GmbH. https://doi.org/10.5194/hess-2022-186

Fetter, C.W., Kreamer, D. (2022). Applied Hydrogeology, fifth edition, Prentice Hall, Upper Saddle River, New Jersey.

Freeze, R.A., and Cherry, J.A. (1979). Groundwater. Prentice Hall, Inc. Englewood Cliffs, New Jersey.

Geologic map of the Aspen quadrangle, Pitkin County, Colorado. (1971). US Geological Survey. https://doi.org/10.3133/gq933

Hare, D. K., Helton, A. M., Johnson, Z. C., Lane, J. W., & Briggs, M. A. (2021). Continental-scale analysis of shallow and deep groundwater contributions to streams. In Nature Communications (Vol. 12, Issue 1). Springer Science and Business Media LLC. https://doi.org/10.1038/s41467-021-21651-0

Hewlett, J.D. (1961). Soil Moisture as a source of base flow from steep mountain watersheds, *U.S. Department of Agriculture*.

Kolm, K.E. and van der Heijde, P.K.M (2011). Hydrologic and Environmental Systems Analysis and Formulation of Conceptual Models for the Central Roaring Fork Tributaries (CRFT), Pitkin County, Colorado, *Integral Consulting*, Louisville, CO.

Lilly, J.O. (2016). A GIS Approach to Modeling Groundwater Levels in the Mississippi River Valley Alluvial Aquifer (2016). Theses and Dissertations. 1827.

Miller, M. P., Susong, D. D., Shope, C. L., Heilweil, V. M., & Stolp, B. J. (2014). Continuous estimation of baseflow in snowmelt-dominated streams and rivers in the Upper Colorado River Basin: A chemical hydrograph separation approach. In Water Resources Research (Vol. 50, Issue 8, pp. 6986–6999). American Geophysical Union (AGU). https://doi.org/10.1002/2013wr014939

Miller, O. L., Miller, M. P., Longley, P. C., Alder, J. R., Bearup, L. A., Pruitt, T., Jones, D. K., Putman, A. L., Rumsey, C. A., & McKinney, T. (2021). How Will Baseflow Respond to Climate Change in the Upper Colorado River Basin? In Geophysical Research Letters (Vol. 48, Issue 22). American Geophysical Union (AGU). https://doi.org/10.1029/2021gl095085

Nathan, R. J., and T. A. McMahon (1990). Evaluation of automated techniques for base flow and recession analysis, *Water Resour. Res.*, **26**, 1465–1473, doi:10.1029/WR026i007p01465.

O'Keefe, T. and Hoffmann, L. (2007). Roaring Fork Watershed Inventory, *Roaring Fork Conservancy,* Basalt, Colorado.

Pinder, G. F., and J. F. Jones (1969). Determination of the ground-water component of peak discharge from the chemistry of total runoff, *Water Resour. Res.*, **5**, 438–445, doi:10.1029/WR005i002p00438.

Prather, M., G. Flato, P. Friedlingstein, C. Jones, J.-F. Lamarque, H. Liao and P. Rasch (2013). IPPC Annex II: Climate System Scenario Tables. In *Climate Change 2013*. Cambridge University Press, Cambridge, United Kingdom and New York, NY, USA.

Rumsey, C. A., Miller, M. P., Susong, D. D., Tillman, F. D., & Anning, D. W. (2015). Regional scale estimates of baseflow and factors influencing baseflow in the Upper Colorado River Basin. In Journal of Hydrology: Regional Studies (Vol. 4, pp. 91–107). Elsevier BV. https://doi.org/10.1016/j.ejrh.2015.04.008

Rumsey, C. A., Miller, M. P., Schwarz, G. E., Hirsch, R. M., & Susong, D. D. (2017). The role of baseflow in dissolved solids delivery to streams in the Upper Colorado River Basin. In Hydrological Processes (Vol. 31, Issue 26, pp. 4705–4718). Wiley. https://doi.org/10.1002/hyp.11390

The Climate Toolbox (2023). Future Climate Scatter, *University of California Merced*, Merced, CA

Sanderson, J. S., Rowan, N., Wilding, T., Bledsoe, B. P., Miller, W. J., & Poff, N. L. (2011). GETTING TO SCALE WITH ENVIRONMENTAL FLOW ASSESSMENT: THE WATERSHED FLOW EVALUATION TOOL. In River Research and Applications (Vol. 28, Issue 9, pp. 1369–1377). Wiley. https://doi.org/10.1002/rra.1542

Sibson, R. (1981). "A Brief Description of Natural Neighbor Interpolation," chapter 2 in *Interpolating Multivariate Data*. New York: John Wiley & Sons, . 21–36.

Schmidt, J.C., Yackulic, C.B., and Kuhn, E. (2023). The Colorado River water crisis: Its origin and the future: WIREs Water, v. 10, doi:10.1002/wat2.1672.

U.S. Geological Survey (2023) National Groundwater Monitoring Network: https://cida.usgs.gov/ngwmn/

U.S. Geological Survey (2023) National Water Information System: https://waterdata.usgs.gov/nwis

U.S. Geological Survey (2023) StreamStats: https://streamstats.usgs.gov/ss/

U.S. Geological Survey (2023) Watershed Boundary Dataset: https://www.usgs.gov/national-hydrography/watershed-boundary-dataset

U.S. Bureau of Reclamation (2012). Colorado River Basin water supply and demand study, study report, 95 pp., U.S. Dep. of the Inter., Washington, D. C. [Available at http://www.usbr.gov/lc/region/programs/crbstudy/finalreport/studyrpt.html.]

Western Regional Climate Center (1980). Independence Pass 5 SW, Colorado (054270), *Desert Research Institute,* Reno, Nevada

IX. APPENDIX A

StationID	Latitude	Longitude	January Soil Moisture (m3/m3)	February Soil Moisture (m3/m3)	March Soil Moisture (m3/m3)	April Soil Moisture (m3/m3)	May Soil Moisture (m3/m3)	June Soil Moisture (m3/m3)	July Soil Moisture (m3/m3)	August Soil Moisture (m3/m3)	September Soil Moisture (m3/m3)	October Soil Moisture (m3/m3)	November Soil Moisture (m3/m3)	December Soil Moisture (m3/m3)
iron1	39.22083	-106.913	0.13	0.13	0.17	0.28	0.27	0.23	0.15	0.12	0.11	0.11	0.12	0.13
iron2	39.20015	-106.801	0.14	0.14	0.16	0.20	0.20	0.15	0.13	0.11	0.11	0.13	0.15	0.14
iron3	39.3794	-107.09	0.49	0.51	0.52	0.50	0.46	0.54	0.69	0.70	0.70	0.69	0.61	0.51
iron5	39.54418	-107.341	0.22	0.26	0.26	0.22	0.20	0.14	0.12	0.10	0.13	0.12	0.18	0.16
iron6	39.17067	-106.799	0.19	0.20	0.24	0.26	0.24	0.15	0.09	0.10	0.10	0.12	0.15	0.18
iron7	39.17114	-106.799	0.34	0.34	0.36	0.45	0.41	0.39	0.34	0.29	0.29	0.30	0.33	0.34
iron8	39.47217	-107.222	0.25	0.27	0.31	0.30	0.27	0.25	0.24	0.26	0.26	0.26	0.26	0.26
iron9	39.10694	-106.574	0.10	0.10	0.10	0.10	0.23	0.30	0.29	0.16	0.10	0.13	0.13	0.11

X.   APPENDIX B

Transect Distance (m)	Change In Groundwater Level (m)	Hydraulic Gradient
24700	947	0.03834
27740	449	0.016186
17700	481	0.027175
48400	845	0.017459
19500	680	0.034872
19400	520	0.026804
14300	400	0.027972
9000	160	0.017778
13600	290	0.021324
24400	570	0.023361

Hydraulic Gradients for Natural Neighbor Interpolation (superset)

Transect Distance (m)	Change in Groundwater Level (m)	Hydraulic Gradient
24800	814	0.032823
27300	914	0.03348
22000	500	0.022727
13150	285	0.021673
51800	880	0.016988
10660	510	0.047842
26300	490	0.018631
18500	520	0.028108
18680	530	0.028373

Hydraulic Gradients for Bayesian Empirical Kriging (superset)

Transect Distance (m)	Change in Groundwater level (m)	Hydraulic Gradient
24,800	900	0.036290323
26050	825	0.031669866
20900	800	0.038277512
17230	475	0.027568195
33290	375	0.011264644
16000	550	0.034375
7500	150	0.02
13130	200	0.015232292

Hydraulic Gradients for Generic Contouring Tool (superset)

XI.　　APPENDIX C

Doc #	Permit #	Year Tested	SWL Prior to Test (ft)	Length of Test (hours)	Sustained Yield (gpm)	Final Water Level (ft)	Depth to Bedrock (b) (ft)	Drawdown	Latitude	Longitude	Specific Capacity	Transmissivity (gpm/ft)	Transmissivity (gpd/ft)	Transmissivity (m2/d)	Hydraulic Conductivity (m/d)	Hydraulic Conductivity (m/s)
DWR 1441192	119062	1983	25.00	4.00	15.00	25.20		0.20	39.15	-106.78	75.00	112500.00	162000000.00	1397.22	35.26	2.45E-02
DWR 1672793	49450-F	1986	95.00	2.00	12.00	95.17		0.17	39.15	-106.78	70.59	105882.35	152470588.24	1315.03	33.19	2.30E-02
DWR 1672793	49450-F	1986	95.00	2.00	12.00	95.17		0.17	39.15	-106.78	70.59	105882.35	152470588.24	1315.03	33.19	2.30E-02
DWR 1001469	259980	2005	46.42		15.00	46.79		0.37	39.13	-106.76	40.54	60810.81	87567567.57	755.25	19.06	1.32E-02
DWR 2268206	75572-F	2007	32.10		17.00	33.60		1.50	39.16	-106.79	11.33	17000.00	24480000.00	211.14	5.33	3.70E-03
DWR 1482647	147731	1987	12.00	3.00	10.00	13.00		1.00	39.15	-106.79	10.00	15000.00	21600000.00	186.30	4.70	3.26E-03
DWR 1487676	151897-A	1988	4.00	2.00	15.00	6.00		2.00	39.15	-106.79	7.50	11250.00	16200000.00	139.72	3.53	2.45E-03
DWR 1540917	195151	1999	16.00	2.00	15.00	18.00		2.00	39.15	-106.78	7.50	11250.00	16200000.00	139.72	3.53	2.45E-03
DWR 999039	253551-A	2005	16.00		15.00	18.92		2.92	39.15	-106.78	5.14	7705.48	11095890.41	95.70	2.42	1.68E-03
DWR 1502659	141055	1985	15.00		25.00	20.00		5.00	39.17	-106.79	5.00	7500.00	10800000.00	93.15	2.35	1.63E-03
DWR 1431579	109450	1980	4.00	2.00	40.00	12.00		8.00	39.15	-106.79	5.00	7500.00	10800000.00	93.15	2.35	1.63E-03
DWR 1142913	140843-A	2000	43.50		15.00	46.71		3.21	39.15	-106.78	4.67	7009.35	10093457.94	87.05	2.20	1.53E-03
DWR 1142913	140843	1985	43.50	5.00	15.00	46.71	85.00	3.21	39.15	-106.78	4.67	7009.35	10093457.94	87.05	2.20	1.53E-03
DWR 1474380	140843	1985	58.00	5.00	31.00	65.00		7.00	39.15	-106.79	4.43	6642.86	9565714.29	82.50	2.08	1.45E-03
DWR 1474380	140843	1987	58.00	2.00	31.00	65.00		7.00	39.15	-106.78	4.43	6642.86	9565714.29	82.50	2.08	1.45E-03
DWR 148354	148530	1985	85.50	5.00	8.00	87.50		2.00	39.15	-106.78	4.00	6000.00	8640000.00	74.52	1.88	1.31E-03
DWR 148354	148530	1987	85.50	2.00	8.00	87.50		2.00	39.15	-106.78	4.00	6000.00	8640000.00	74.52	1.88	1.31E-03
DWR 940842	239426	2002	11.50		15.00	15.33		3.83	39.13	-106.75	3.92	5874.67	8459530.03	72.96	1.84	1.28E-03
DWR 2955473	302639	2002	11.50		15.00	15.33		3.83	39.13	-106.75	3.92	5874.67	8459530.03	72.96	1.84	1.28E-03
DWR 1474380	140843	1985	60.00	2.00	30.00	68.00	85.00	8.00	39.15	-106.78	3.75	5625.00	8100000.00	69.86	1.76	1.22E-03
DWR 2473624	271883-A	2012	51.00		15.00	55.17		4.17	39.16	-106.79	3.60	5395.68	7769784.17	67.01	1.69	1.17E-03
DWR 1399545	80050	1975	72.00	4.00	18.00	78.00		6.00	39.16	-106.79	3.00	4500.00	6480000.00	55.89	1.41	9.79E-04
DWR 1525438	182373	1995	49.00		8.00	51.67		2.67	39.18	-106.80	3.00	4494.38	6471910.11	55.82	1.41	9.78E-04
DWR 2626817	718137-F	1978	12.00	2.00	28.00	22.00		10.00	39.29	-106.92	2.80	4200.00	6048000.00	52.16	1.32	9.14E-04
DWR 1416987	96690	1978	12.00	2.00	28.00	22.00		10.00	39.29	-106.92	2.80	4200.00	6048000.00	52.16	1.32	9.14E-04
DWR 1472445	139239	1985	14.00	3.00	20.00	22.00		8.00	39.16	-106.79	2.50	3750.00	5400000.00	46.57	1.18	8.16E-04
DWR 1671943	048639-F	1996	16.33		15.00	22.75		6.42	39.42	-107.21	2.34	3504.67	5046728.97	43.53	1.10	7.63E-04
DWR 2626817	78137-F	1978	12.00	2.00	28.00	24.00		12.00	39.29	-106.92	2.33	3500.00	5040000.00	43.47	1.10	7.62E-04
DWR 3269733	80066-F	2018	23.00	2.00	15.00	30.00		7.00	39.30	-106.93	2.14	3214.29	4628571.43	39.92	1.01	7.00E-04
DWR 1399545	80050	1975	51.00	4.00	25.00	64.00		13.00	39.16	-106.79	1.92	2884.62	4153846.15	35.83	0.90	6.28E-04
DWR 1653610	31854-F	1979	32.00	3.00	15.00	40.00		8.00	39.18	-106.78	1.88	2812.50	4050000.00	34.93	0.88	6.12E-04
DWR 3260145	80067-F	2018	42.00	2.00	15.00	52.00		10.00	39.30	-106.93	1.50	2250.00	3240000.00	27.94	0.71	4.90E-04
DWR 2479536	77034-F	2012	12.01		13.00	21.00		8.99	39.18	-106.80	1.45	2169.08	3123470.52	26.94	0.68	4.72E-04
DWR 1424270	102823	1979	45.00	2.00	20.00	59.00		14.00	39.29	-106.91	1.43	2142.86	3085714.29	26.61	0.67	4.66E-04
DWR 1476789	142943	1986	72.00	2.00	15.00	84.00		12.00	39.16	-106.79	1.25	1875.00	2700000.00	23.29	0.59	4.08E-04
DWR 2479536	77034-F	2012	12.00	2.00	12.00	23.00		11.00	39.18	-106.80	1.09	1636.36	2356363.64	20.32	0.51	3.56E-04
DWR 2550723	119062-A	2012	32.00		15.00	46.00		14.00	39.15	-106.78	1.07	1607.14	2314285.71	19.96	0.50	3.50E-04
DWR 1355736	34988	1968		3.00	10.00			10.00	39.17	-106.79	1.00	1500.00	2160000.00	18.63	0.47	3.26E-04
DWR 2479533	77031-	2012	12.85		8.00	21.00		8.15	39.18	-106.80	0.98	1472.39	2120245.40	18.29	0.46	3.20E-04
DWR 1124290	05321L-F	2001	11.00		15.00	26.75		15.75	39.15	-106.78	0.95	1428.57	2057142.86	17.74	0.45	3.11E-04
DWR 2479533	77031-	2012	13.00		8.00	23.00		10.00	39.18	-106.80	0.80	1200.00	1728000.00	14.90	0.38	2.61E-04
DWR 1422680	101445	1979	2.00	0.50	20.00	27.00		25.00	39.15	-106.79	0.80	1200.00	1728000.00	14.90	0.38	2.61E-04
DWR 1394572	74951	1974	22.00	2.00	20.00	50.00		28.00	39.16	-106.78	0.71	1071.43	1542857.14	13.31	0.34	2.33E-04
DWR 1389560	69176	1975	40.00	2.00	40.00	100.00		60.00	39.15	-106.79	0.67	1000.00	1440000.00	12.42	0.31	2.18E-04
DWR 1669123	046115-F	1988	100.25		15.00	123.50		23.25	39.15	-106.78	0.65	967.74	1393548.39	12.02	0.30	2.11E-04
DWR 2398543	70305-F	1988	16.33		8.00	31.50		15.17	39.30	-106.92	0.53	791.03	1139090.31	9.82	0.25	1.72E-04
DWR 1465837	133441	2012	185.00	2.00	10.00	210.00	180.00	25.00	39.16	-106.79	0.40	600.00	864000.00	7.45	0.19	1.31E-04
DWR 2479529	77027-F	1983	12.56		2.80	20.00		7.44	39.18	-106.80	0.38	564.52	812903.23	7.01	0.18	1.23E-04
DWR 1424272	102825-	2012	16.00	3.00	7.00	40.00		24.00	39.18	-106.80	0.29	437.50	630000.00	5.43	0.14	9.52E-05
DWR 148354	148330	1979	86.00	2.00	7.00	111.00		25.00	39.15	-106.78	0.28	420.00	604800.00	5.22	0.13	9.14E-05
DWR 2479529	77027-F	1987	11.00	2.00	2.80	23.00		12.00	39.18	-106.80	0.23	350.00	504000.00	4.35	0.11	7.62E-05
DWR 1148294	23661	2012	65.00	1.00	15.00	135.00		70.00	39.16	-106.79	0.21	321.43	462857.14	3.99	0.10	7.00E-05
DWR 1301913	144526-A	2001	30.00	2.00	12.00	90.00		60.00	39.16	-106.79	0.20	300.00	432000.00	3.73	0.09	6.53E-05
DWR 2479531	77029-	2000	0.90		0.90	19.00		5.82	39.18	-106.80	0.15	231.96	334020.62	2.88	0.07	5.05E-05
DWR 1355829	35071	2012	13.18		10.00			70.00	39.18	-106.80	0.14	214.29	308571.43	2.66	0.07	4.66E-05
DWR 1442693	120538	1968	70.00	4.00	10.00	150.00		80.00	39.15	-106.78	0.13	187.50	270000.00	2.33	0.06	4.08E-05
DWR 2479533	77029-	1981	12.00	2.00	0.90	23.00		11.00	39.18	-106.80	0.08	122.73	176727.27	1.52	0.04	2.67E-05